Using Deep-Learning Reconstruction on Undersampled k-Space Data

Mostly based on this review

What does MRI even measure?

Some useful terms:

TR - Repetition Time
The amount of time between successive pulse sequences applied to the same slice

TE - Time to Echo
The time between the delivery of the RF pulse and receipt of the echo signal

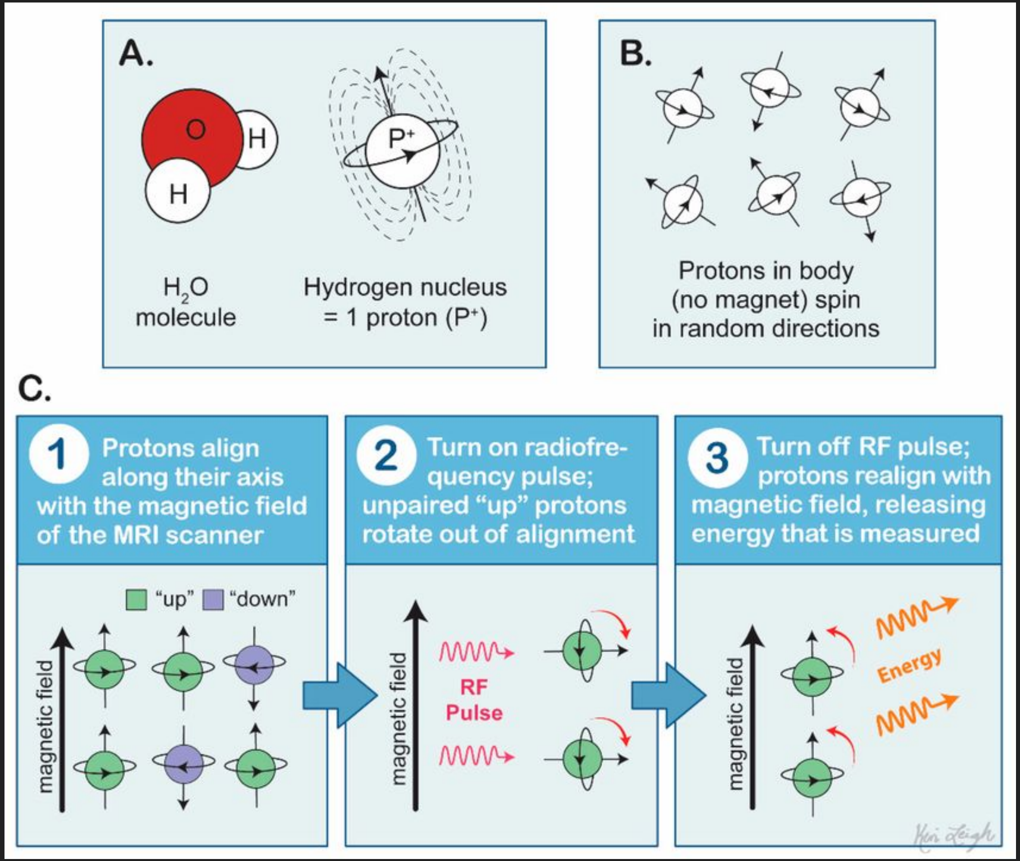

From Fordham, Austin-John, et al. "Differentiating glioblastomas from solitary brain metastases: an update on the current literature of advanced imaging modalities." Cancers 13.12 (2021): 2960.

A brief introduction to K-Space

Data is collected in the
Frequency Domain

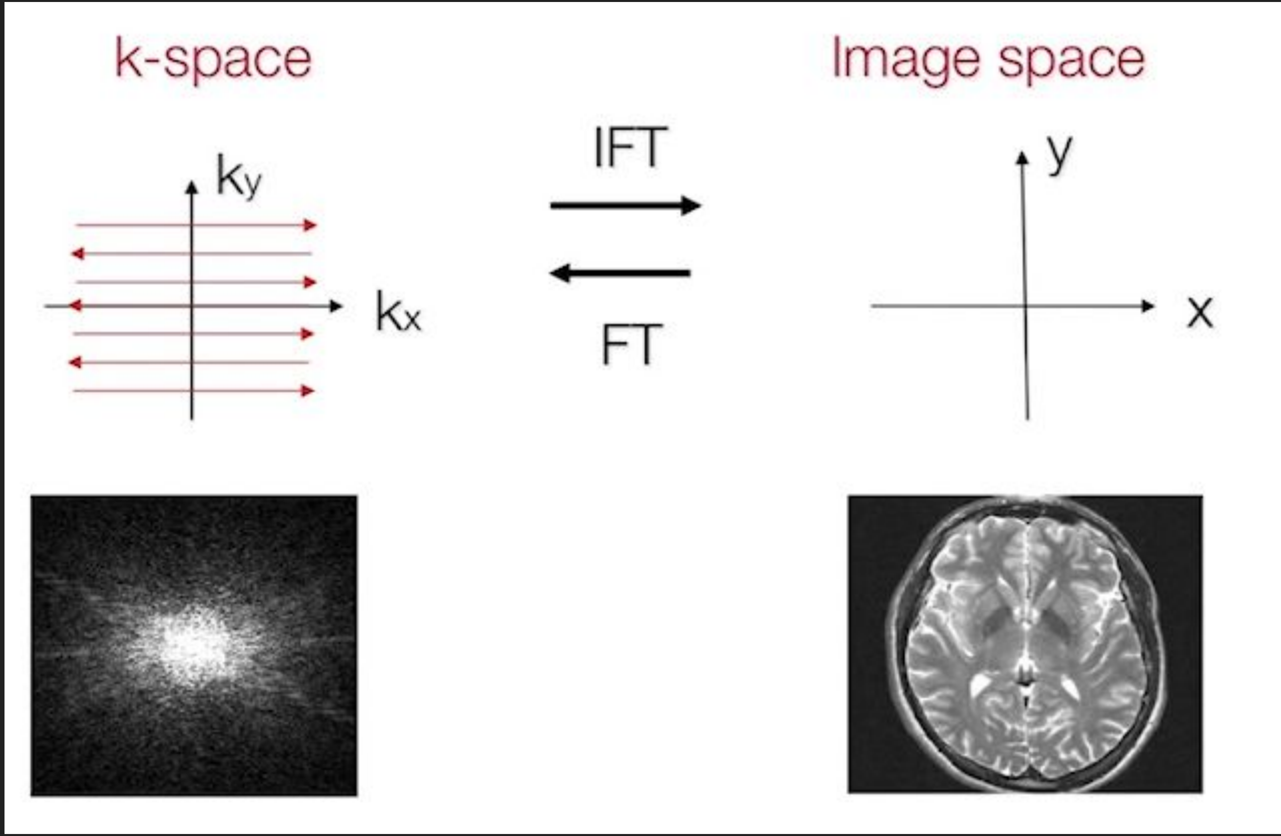

From [Principles of fMRI Part 1, Module 7: K-space]

A brief introduction to K-Space

Data is collected in the **Frequency Domain**

Essentially each point corresponds to a 2-dimensional sinusoid

Location on the plane Determines frequency

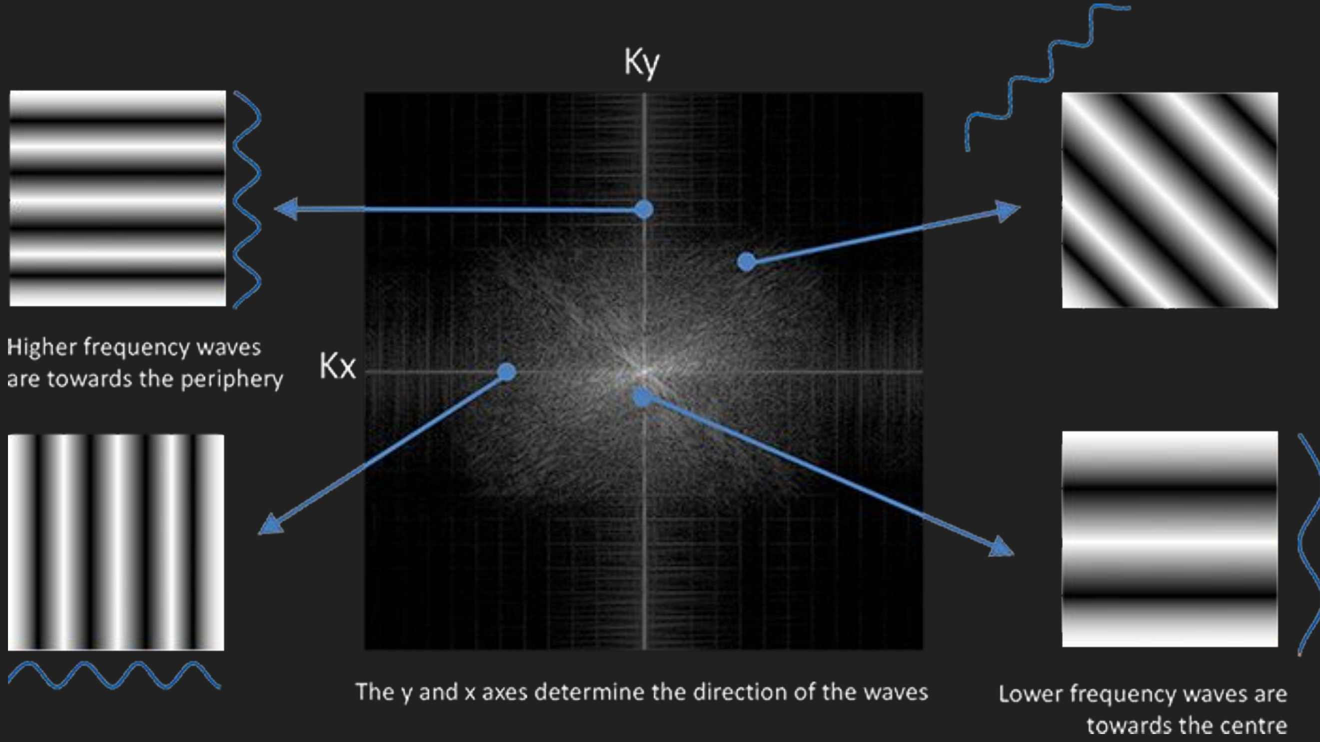

A brief introduction to k-space

Low spatial frequencies correspond to parts of image that change slowly in the image

High spatial frequencies represent small structures on the order of voxel size, such as tissue boundaries

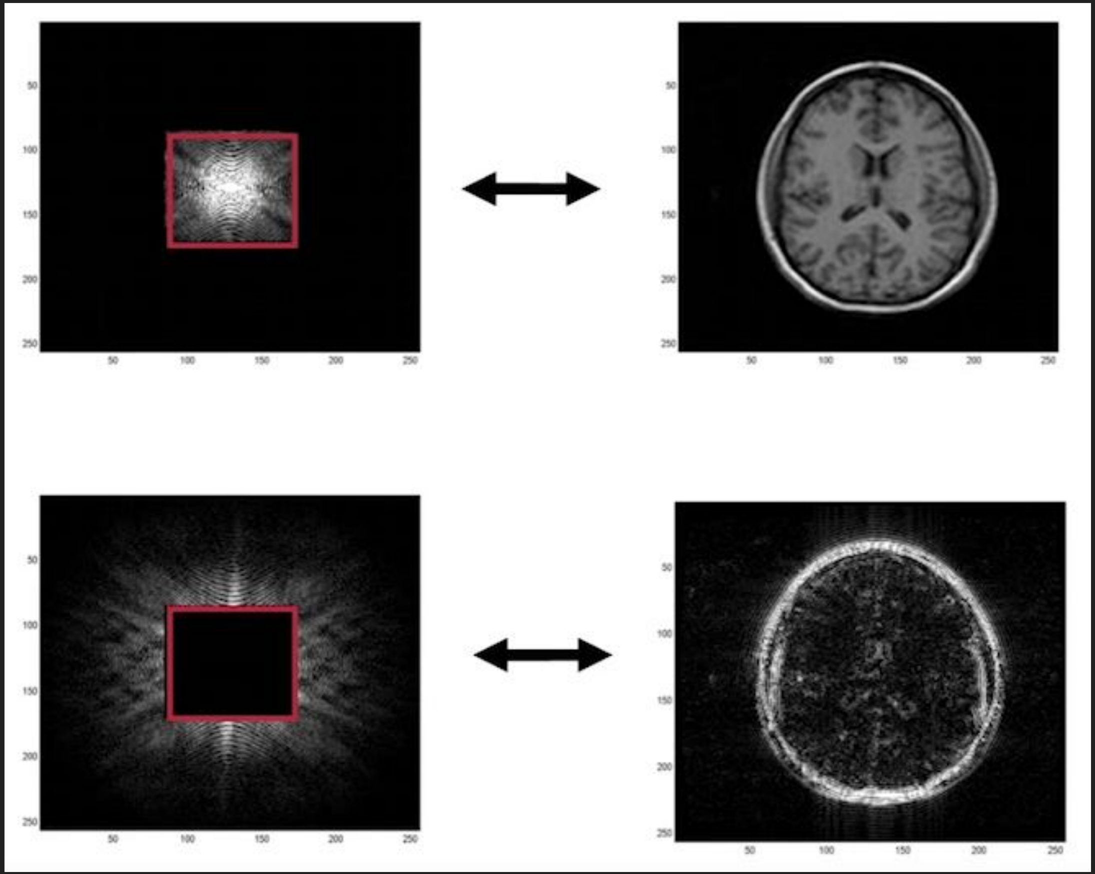

From [Principles of fMRI Part 1, Module 7: K-space]

There are many ways to fill k-space

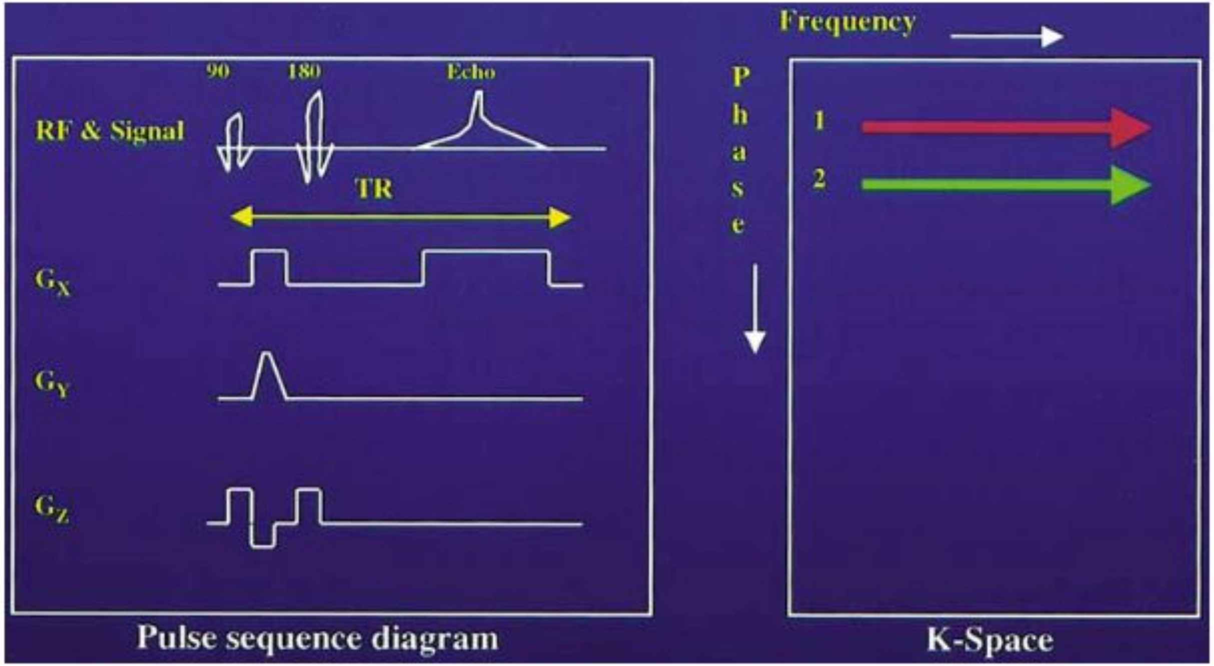

Figure 2. Conventional SE imaging. Within each TR period, the pulse sequence is executed and one line of imaging data or one phase-encoding step is collected. The frequency-encoding gradient (G_x), phase-encoding gradient (G_y), and section-selection gradient (G_z) are shown during one TR period. *RF* = radio frequency.

From [Poustchi-Amin, Mehdi, et al. "Principles and applications of echo-planar imaging: a review for the general radiologist." Radiographics 21.3 (2001): 767-779.]

There are many ways to fill k-space

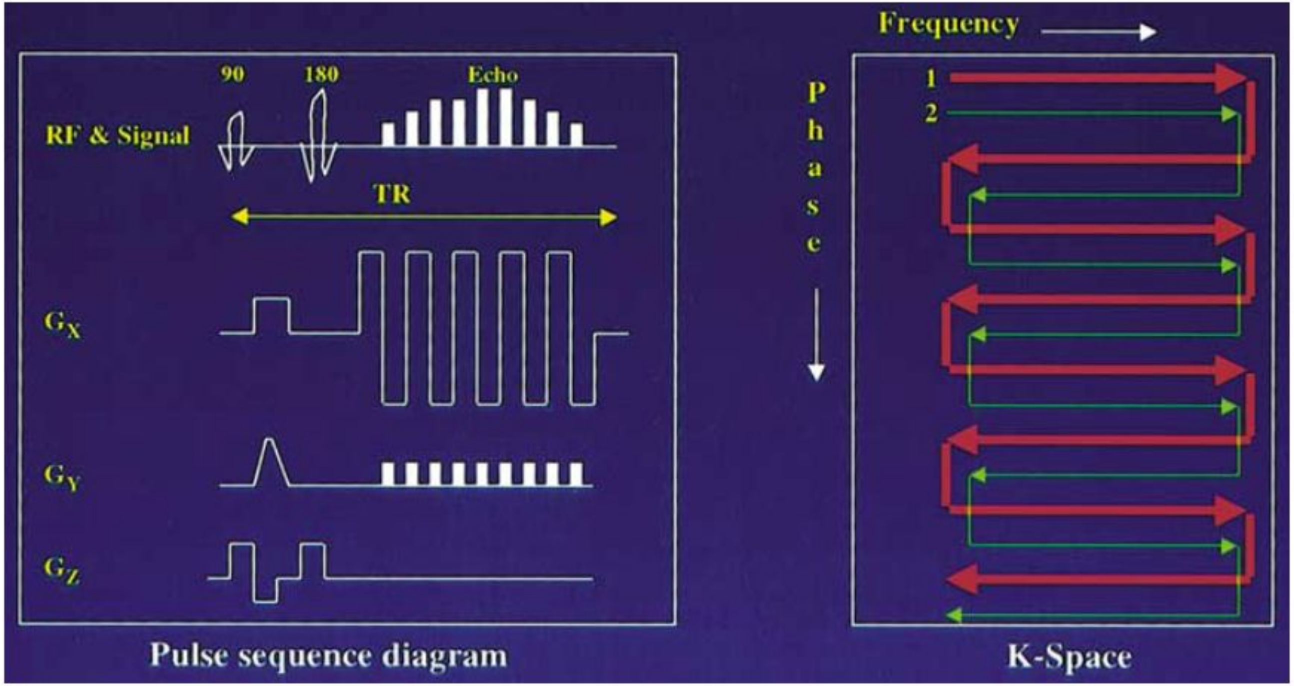

Figure 3. Echo-planar imaging. Within each TR period, multiple lines of imaging data are collected. G_x = frequency-encoding gradient, G_y = phase-encoding gradient, G_z = section-selection gradient.

From [Poustchi-Amin, Mehdi, et al. "Principles and applications of echo-planar imaging: a review for the general radiologist." Radiographics 21.3 (2001): 767-779.]

There are many ways to fill k-space

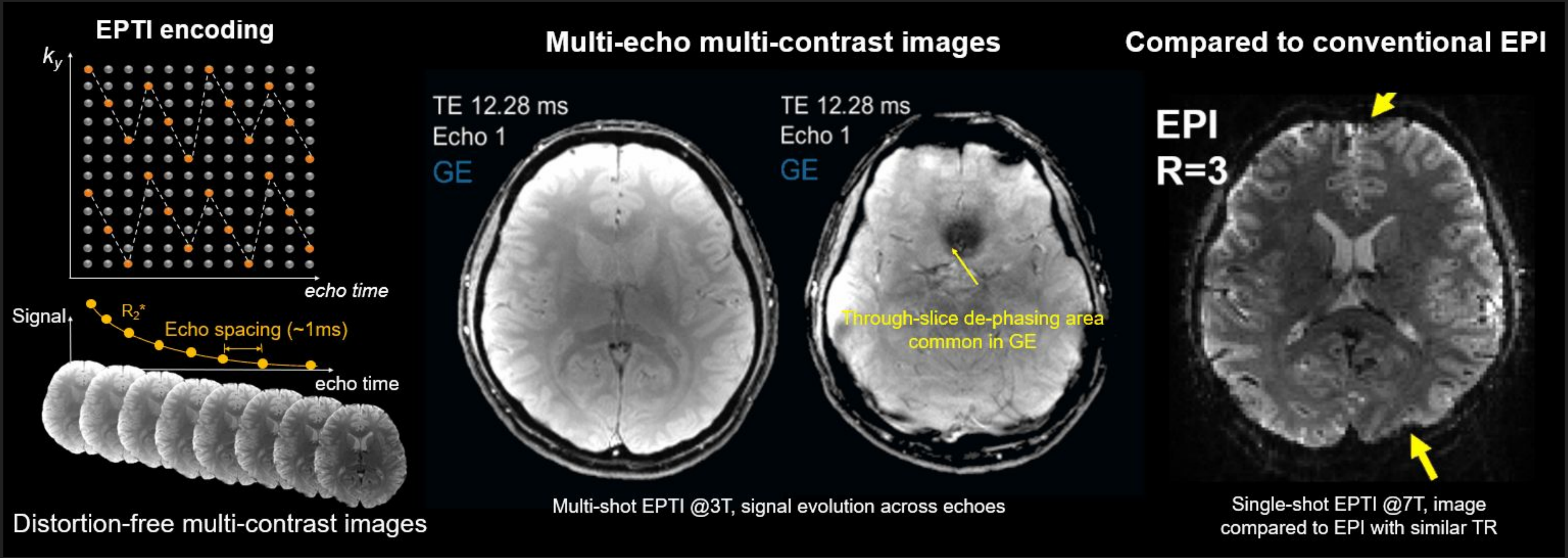

From [Echo-Planar Time-Resolved Imaging]

Undersampling K-Space

Quite a frequent practice. Essentially - we can skip filling in certain parts of K-space and **save time.**

BUT - undersampling introduces artifacts, when we use standard reconstruction methods (just FFT)

The trick is to **exploit relationships** between parts of k-space to reconstruct image using **fewer samples**

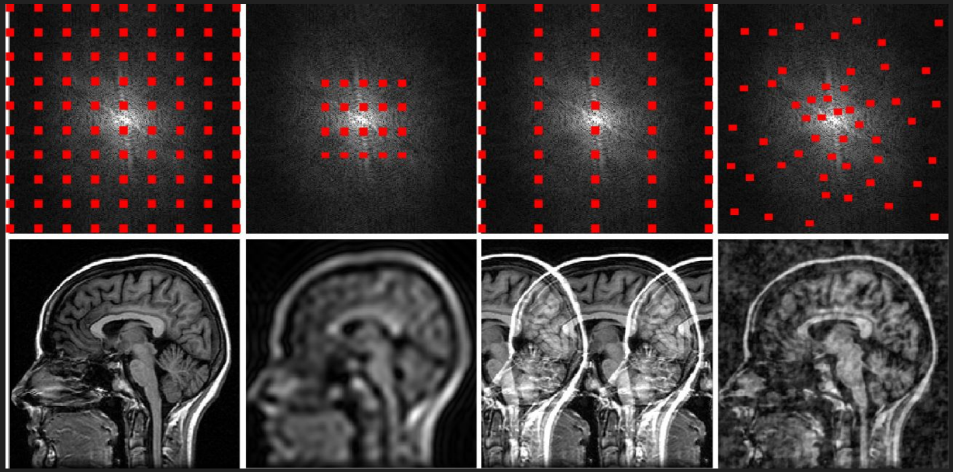

From Lustig, Michael, et al. "Compressed sensing MRI." IEEE signal processing magazine 25.2 (2008): 72-82.

Formulating the Problem

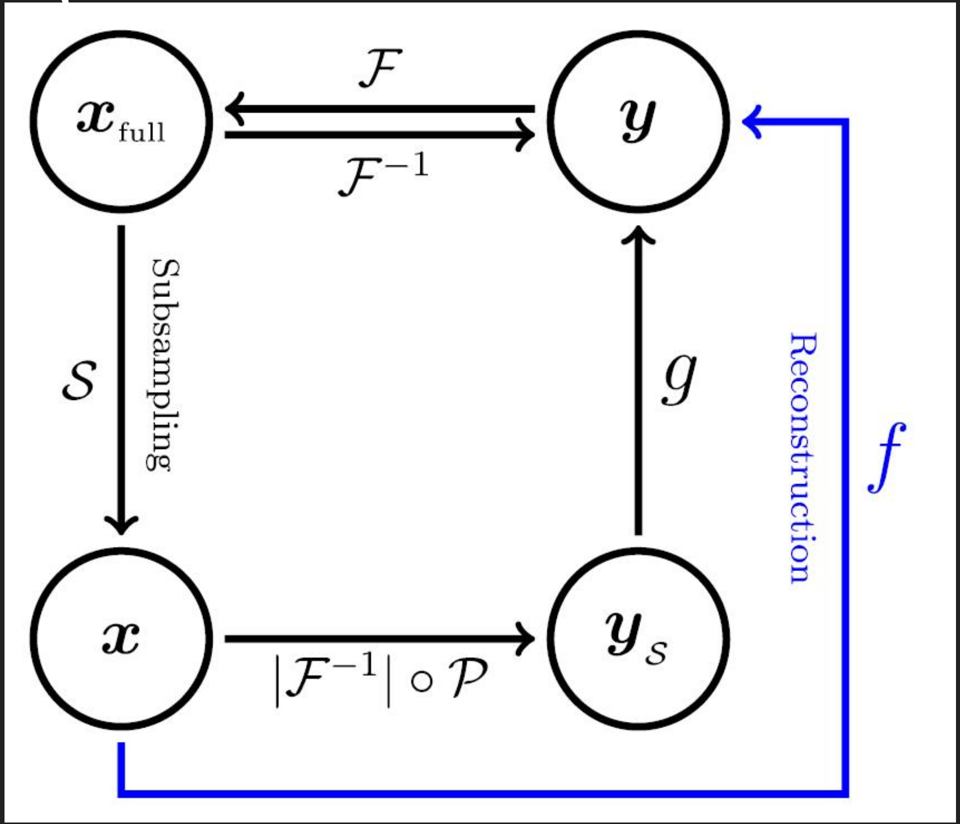

From [Hyun, Chang Min, et al. "Deep learning for undersampled MRI reconstruction." Physics in Medicine & Biology 63.13 (2018): 135007.]

Non-Deep Methods

SENSE *reconstructs* then *corrects*

Sensitivity Encoding (SENSE) - Exploit FOV from multiple coils

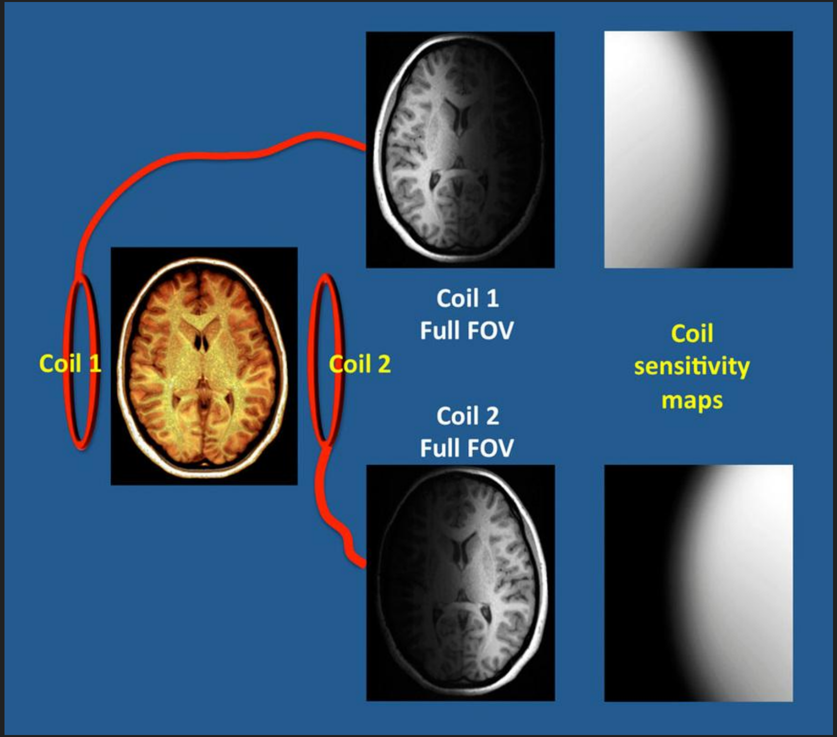

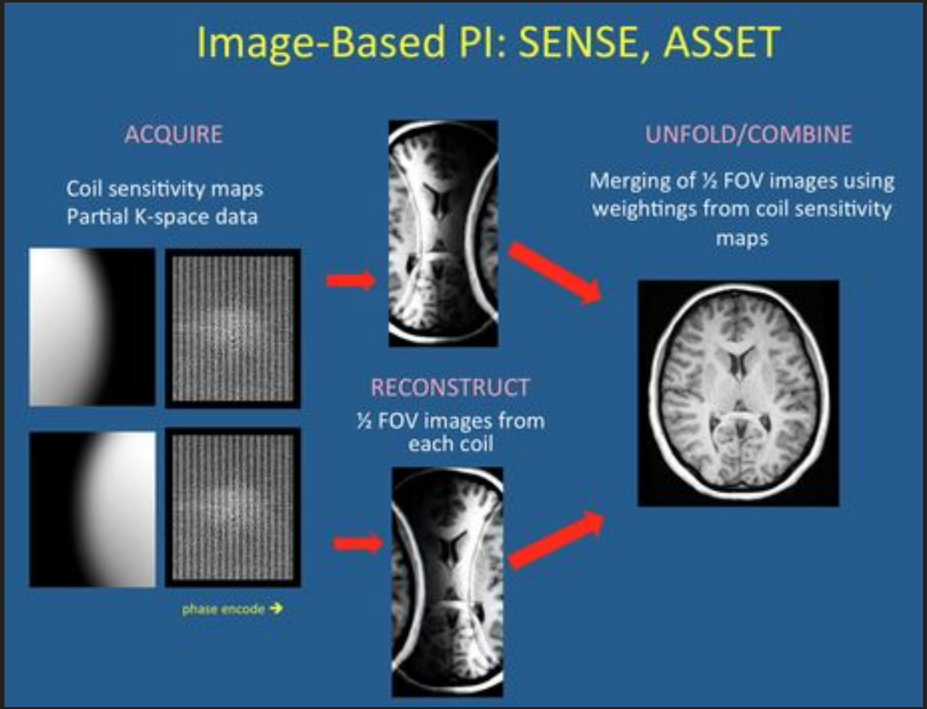

From [How does SENSE/ASSET work? - Questions and Answers in MRI]

Non-Deep Methods

SENSE *reconstructs* then *corrects*

Sensitivity Encoding (SENSE) - Exploit FOV from multiple coils

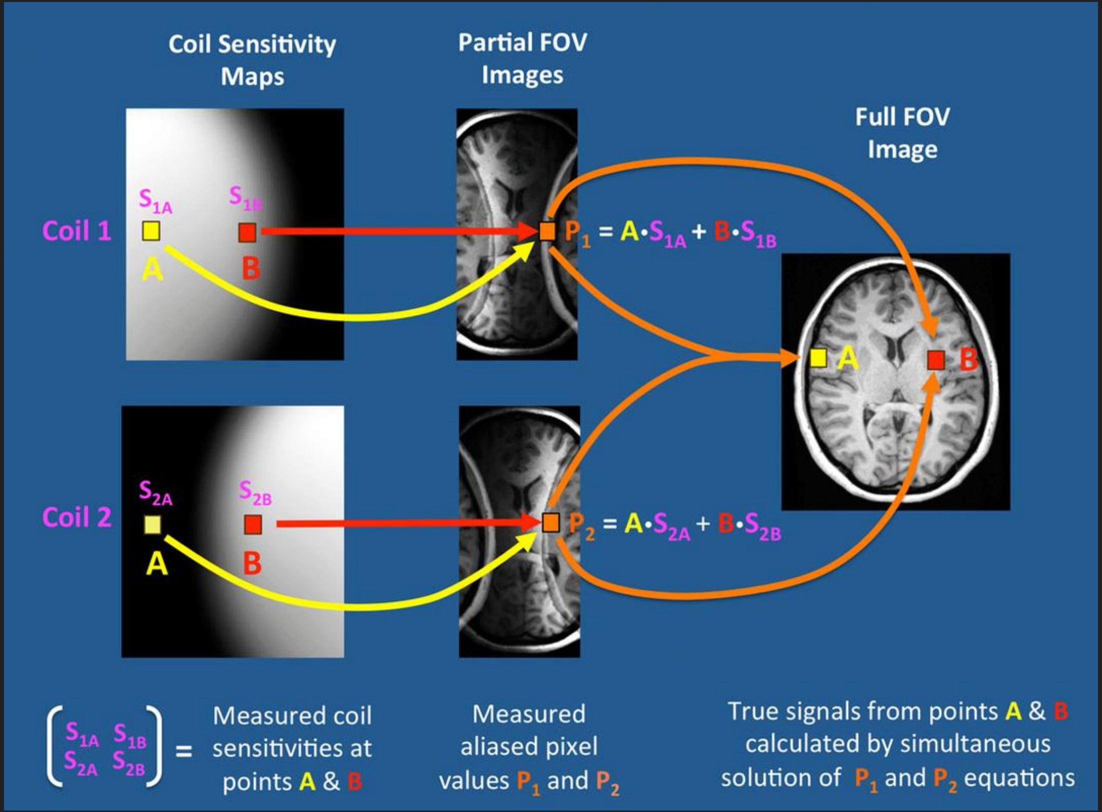

From [How does SENSE/ASSET work? - Questions and Answers in MRI]

Non-Deep Methods

Grappa *corrects* then *reconstructs*

Generalized Autocalibrating Partially Parallel Acquisitions (GRAPPA)

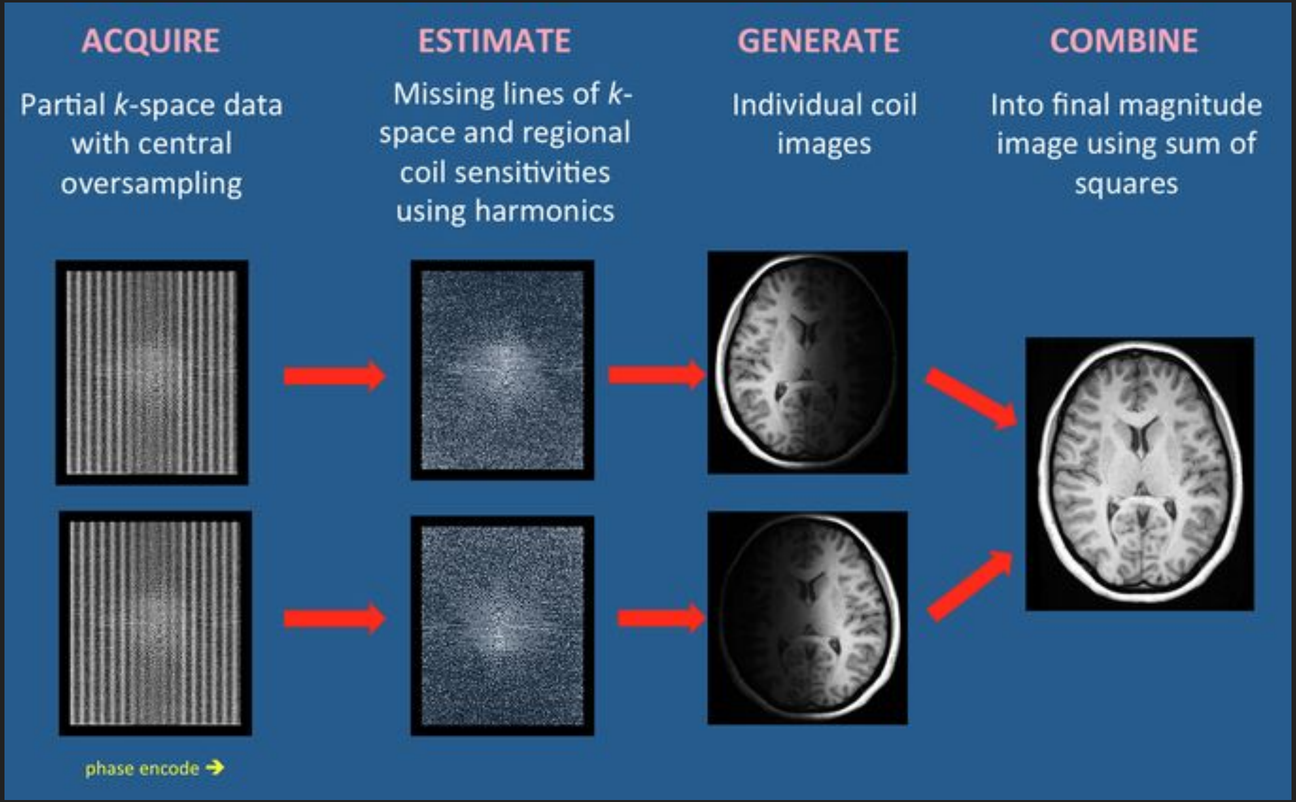

From How Does GRAPPA/ARC work? - Questions and Answers in MRI

Non-Deep Methods

Self-Consistent Parallel Imaging Reconstruction (SPIRiT)

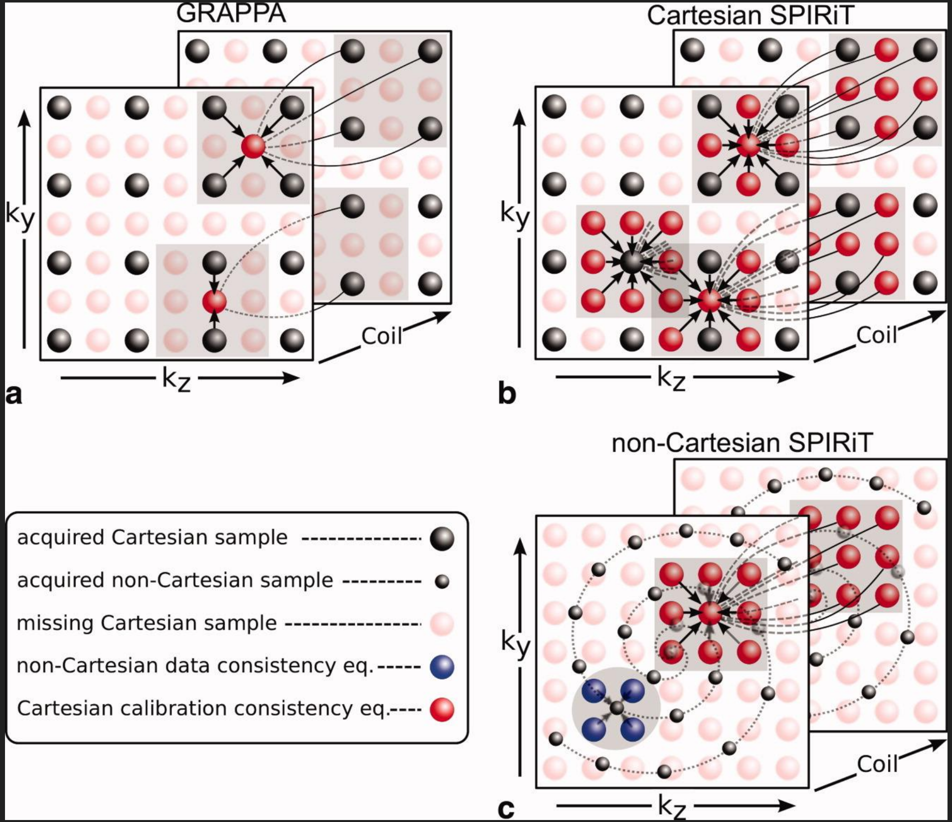

Non-Deep Methods

Compressed Sensing and Parallel Imaging - Exploit Inherent Sparsity

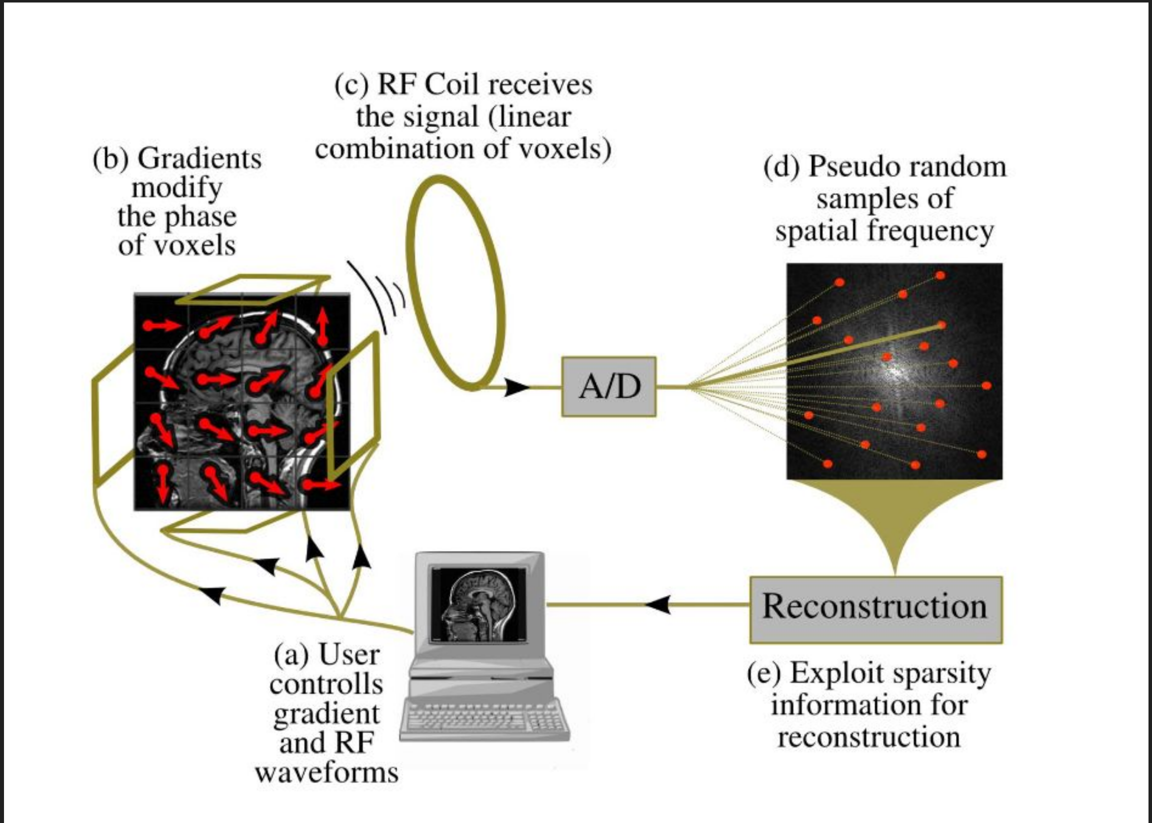

See [Lustig, Michael, et al. "Compressed sensing MRI." IEEE signal processing magazine 25.2 (2008): 72-82.]

Non-Deep Methods

Subspace Reconstruction - [Dong, Zijing, et al. "Echo planar time-resolved imaging with subspace reconstruction and](#)

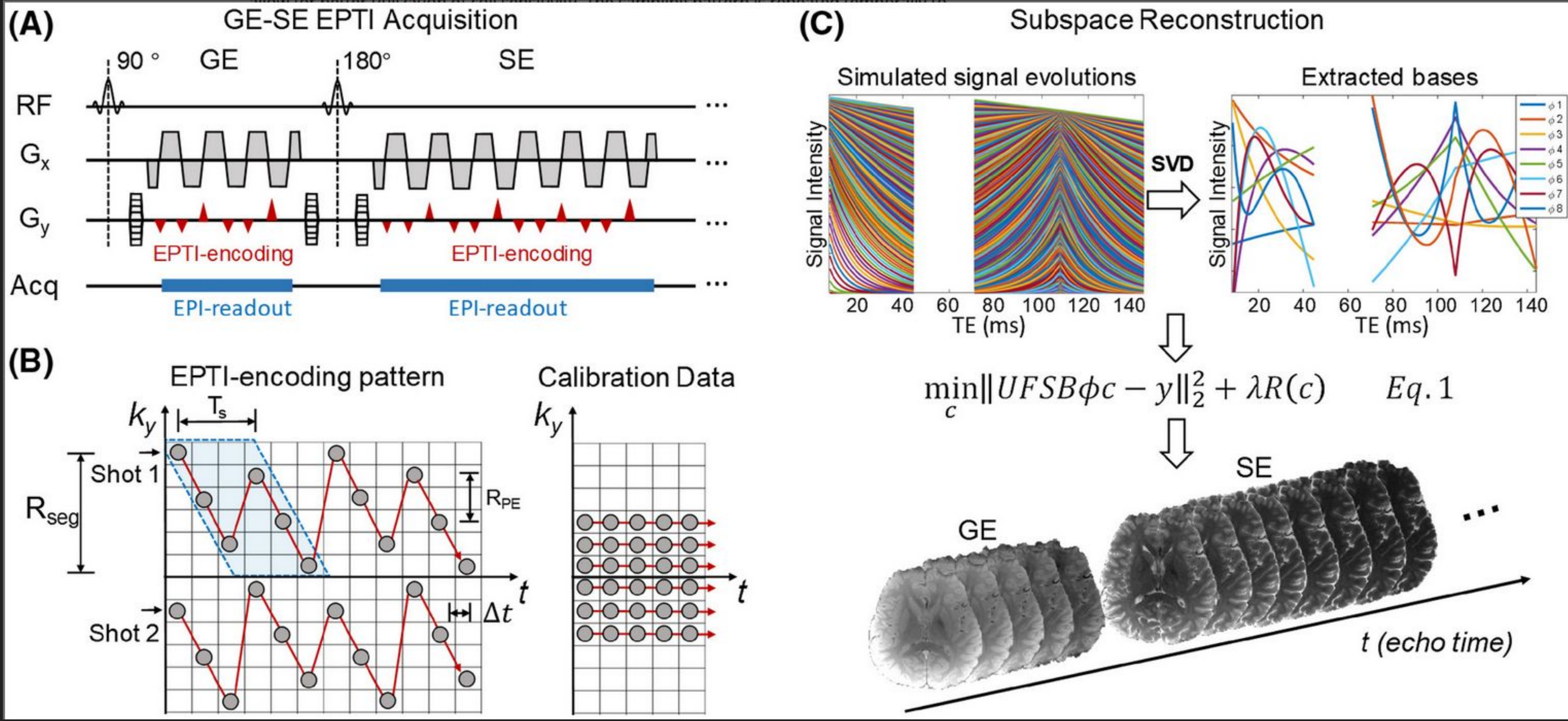

Formulating the Problem (AGAIN)

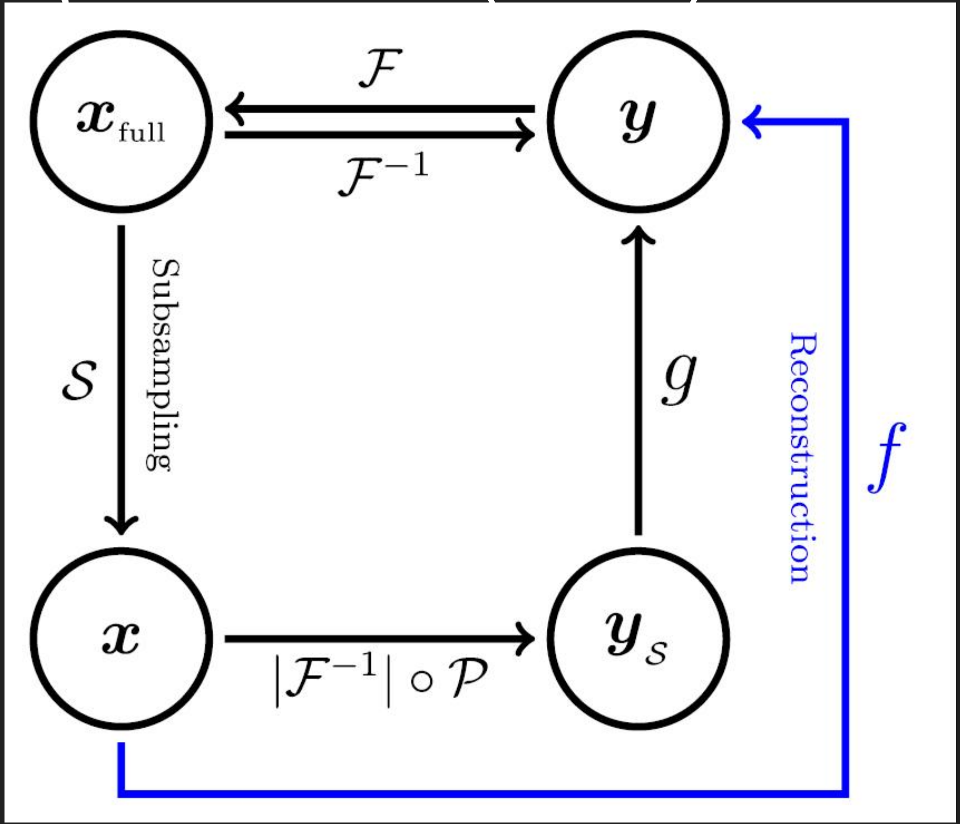

From [Hyun, Chang Min, et al. "Deep learning for undersampled MRI reconstruction." Physics in Medicine & Biology 63.13 (2018): 135007.]

Methodological Overview

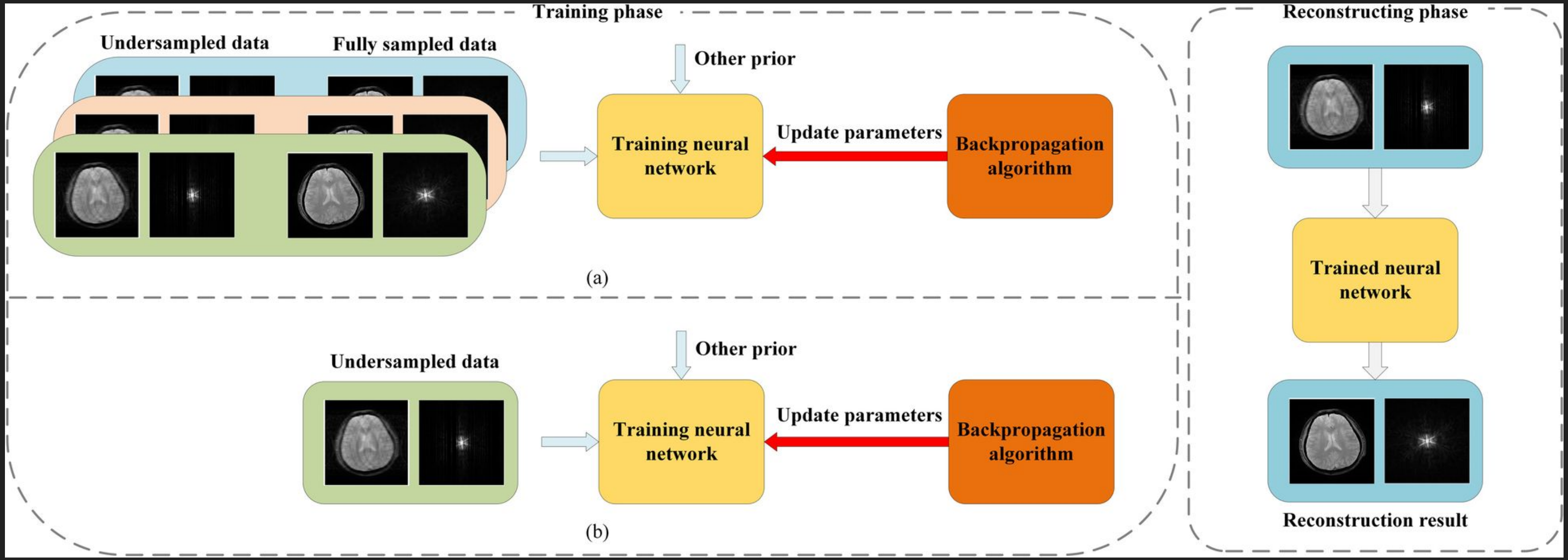

From [Zeng, Gushan, et al. "A review on deep learning MRI reconstruction without fully sampled k-space." BMC Medical Imaging 21.1 (2021): 195.]

There are SO many methods

Figure 11. Number of Published Papers on DL Reconstruction Architectures focusing on Residual Learning (RL), Image Representation using Encoders and Decoders (IR-ED), Data-consistency Layers and Unrolled Networks (DC-UN), Learned Activations and Attention Modules (LA-AM), and Plug-and-play Priors, Diffusion Models, and Bayesian Methods (PDBM).

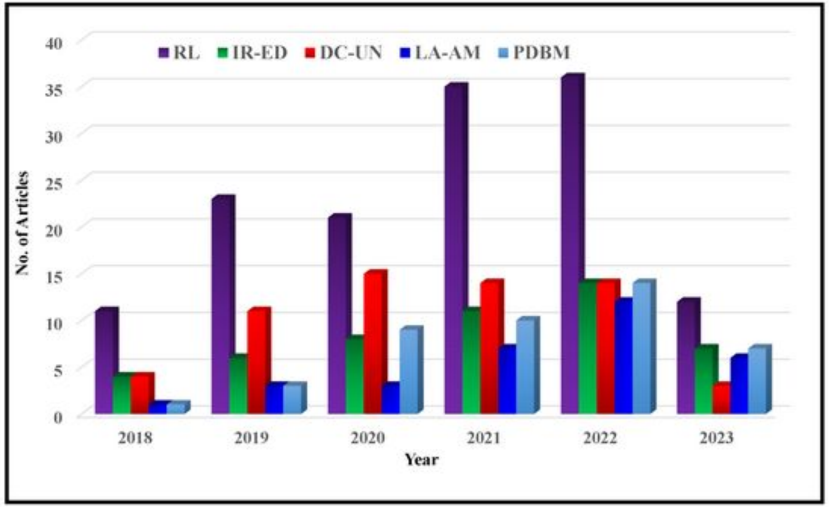

Figure 12. Trends on Improving Reconstruction-Related MRI Applications including Non-Cartesian Reconstruction (NCR), Super-resolution (SR), Joint learning: Coil-sensitivity and Reconstruction (JL-Coil), Joint learning: Sampling and Reconstruction (JL-Samp), Quantitative Mapping (QM), MR Fingerprinting (MRF), and Dynamic MRI (DMRI).

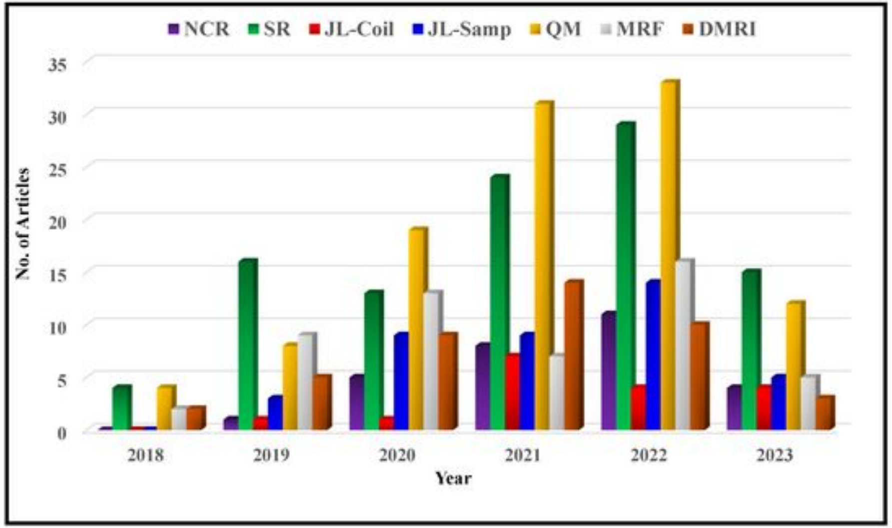

And Many Datasets

Table 7. Features of Popular MRI Reconstruction Datasets.

Ref	Dataset Name	Body Part	Imaging Modality	Additional Features
[111]	BrainWeb	Brain	T1-weighted, T2-weighted	Simulated noise, intensity non-uniformity, and pathology
[112]	FastMRI	Brain, Knee	T1-weighted, PD-weighted	Large-scale dataset, raw k-space data available
[113]	IXI Dataset	Brain	T1-weighted, T2-weighted, PD-weighted	Multi-center data, various imaging sequences
[114]	Calgary-Campinas Public Brain MR Dataset	Brain	T1-weighted, T2-weighted	Multi-coil data, different field strengths (1.5T and 3T)
[115]	ACDC Challenge Dataset	Heart	Cine-MRI	Multi-center cardiac MRI data with ground truth segmentations
[116]	IXI Breast MRI Dataset	Breast	Dynamic Contrast-Enhanced MRI (DCE-MRI)	Breast MRI data with manual segmentations for studying breast cancer

We have some of this data!

Welcome to the fastMRI Dataset

NYU Langone Health

About Us

Here at the Center for Advanced Imaging Innovation and Research (CAI^2R), in the Department of Radiology at NYU School of Medicine and NYU Langone Health, we bring people together to create new ways of seeing. We are committed to the translation of new imaging techniques and technologies into clinical practice, for the improvement of human health. In particular, we are pushing the boundaries of rapid image acquisition and advanced image reconstruction, with the aim of providing uniquely valuable biomedical information to advance the understanding of disease and improve the care of patients.

fastMRI

We are partnering with Facebook AI Research (FAIR) on fastMRI – a collaborative research project to investigate the use of AI to make MRI scans up to 10X faster.

NYU Langone and FAIR are providing open-source AI models, baselines, and evaluation metrics.

The Dataset

The deidentified imaging dataset provided by NYU Langone comprises raw k-space data in several sub-dataset groups. Curation of these data are part of an IRB approved study.

Apply for Access

The application process includes acceptance of the Data Sharing Agreement (found below) and submission of an online application form. The application must include the investigator's institutional affiliation and the proposed uses of the data. NYU fastMRI data may be used for internal research or educational purposes only as described in the data use agreement and may not be redistributed in any way without prior permission.
Read and agree to the data use agreement below to apply for access.

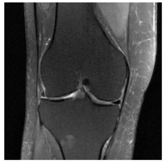

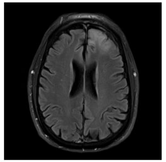

Architectures - ResNets

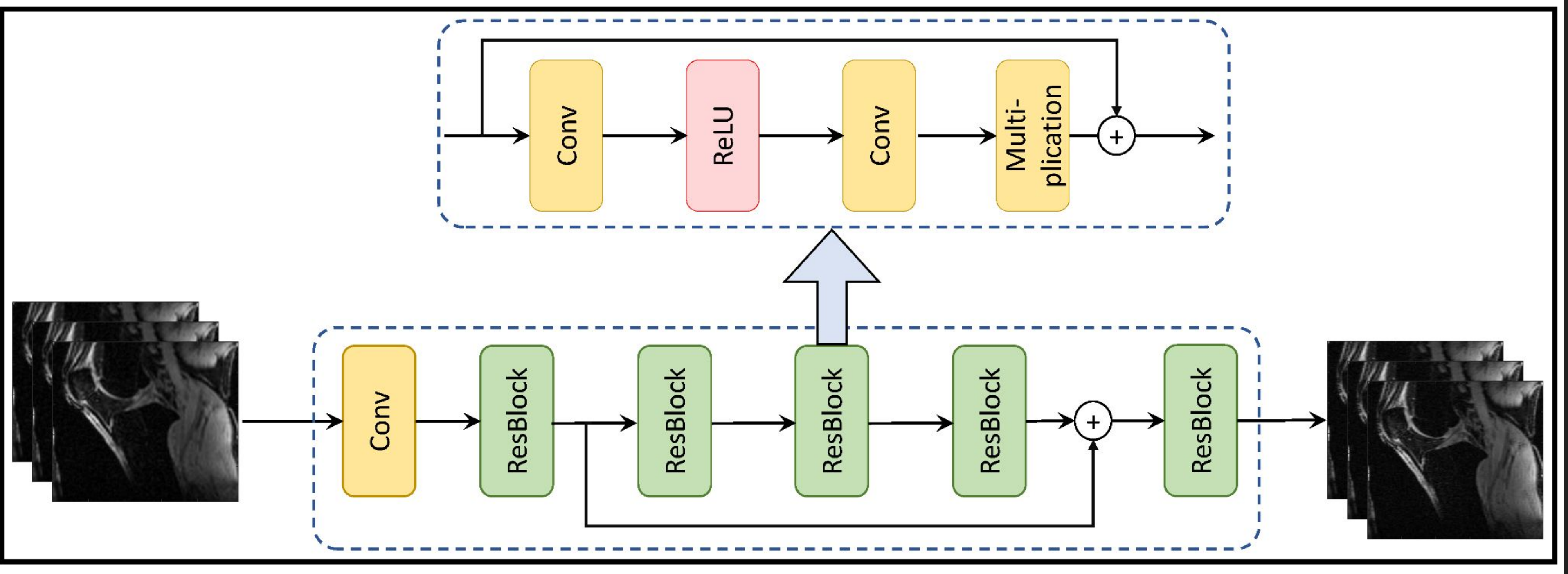

Architectures - ResNets

Table 3. Comparison of Residual Learning (RL)-based MRI Reconstruction Models.

Ref.	Year	Contributions	Unsolved Challenges
[53]	2018	Used deep residual learning network to learn global artifact patterns, and applied dual frame U-net for artifact correction	Potential blurriness due to L2 loss function
[54]	2019	Implemented multi-scale dilated network using global and local residual learnings to preserve image details	Lack of interpretability and explainability
[55]	2019	Introduced an enhanced recursive residual network by incorporating high-frequency feature guidance, dense connections, and an error-correction unit for superior reconstructions with restored structural features	Network depth balancing, challenges in handling 3D image data, and reliance on precomputed coil sensitivity maps for multi-channel MR data
[56]	2020	Employed sub-band residual learning to enhance high-frequency details in low-resolution MR images and a parallel stream for refined image reconstruction	Does not consider 3D structural and spatial details of MRIs
[57]	2020	Utilized residual learning and attention mechanisms within an encoder-decoder network to transform spherical harmonics coefficients in diffusion MRI	Need more comprehensive evaluation to access the effectiveness and robustness of the network
[58]	2020	Utilized a hierarchical architecture, dense local connections, and global skip-connections to enhance signal synthesis and artifact suppression	Limited data size may limit the generalizability and robustness of the model
[59]	2020	Designed a systematic geometric model using bootstrapping and subnetwork aggregation to increase the expressivity of network	Expressivity improvement scheme was only validated on U-Net and the impact of batch normalization was not analyzed
[60]	2022	Developed denoising of 3D fast spin echo MRIs using spatial-variant noise-relevant residual learning	Network retraining required for changing imaging protocols; potential limitations on real patient data, and longer scan time for ground truth images

Architectures - Encoder/Decoders

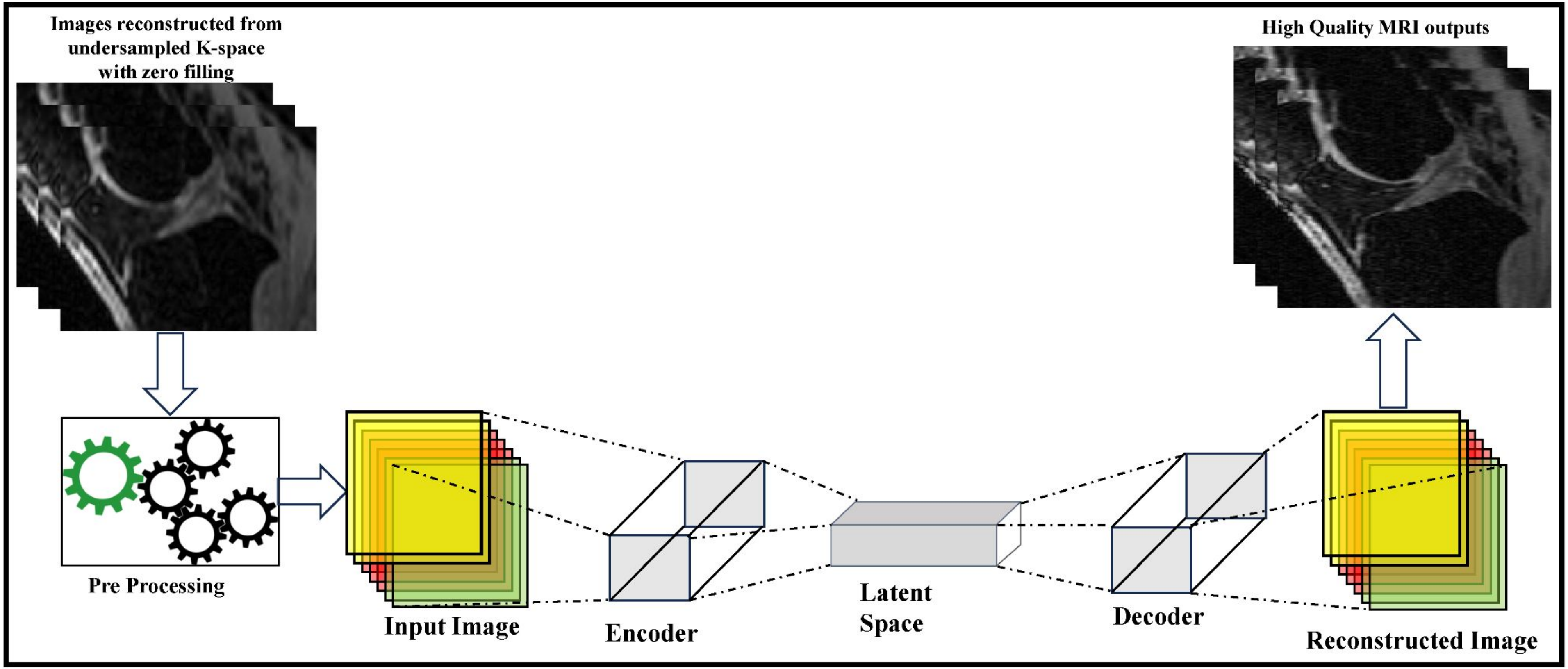

Architectures - Encoder/Decoders

Table 4. Comparison of encoder and decoder-based models.

Ref.	Year	Network	Contributions	Unsolved Challenges
[63]	2019	DISN	Improved MRI reconstruction quality and robustness to misregistration errors	Limited generalization to unseen data and imaging conditions, lack of interpretability and explainability as black box models
[64]	2019	VDDCN	Made the network easy to train using dense connections and alleviated gradient-vanishing problem	Limited generalization to unseen data and imaging conditions, data scarcity and the need for large amounts of labeled training data
[65]	2019	IFR-Net	Improved network capacity with better feature refinement and fully learned parameters	Limited generalization to unseen data and imaging conditions, prone to overfitting
[66]	2020	DECN	Reduced structural reconstruction errors and improved MRI quality	Lack of interpretability and explainability as black-box models, may lead to artifacts and noise
[67]	2020	NISTAD	Reduced reconstruction time, simplified hyperparameter tuning, and a simpler network architecture with fewer parameters	Not efficient for highly undersampled image sequence reconstruction and might not be realistic enough for real clinical scans
[68]	2021	X-net & Y-net	Reduced number of trainable parameters, leading to a more efficient and streamlined model architecture	Lower computational efficiency due to the incorporation of additional network branches and the increased complexity of the model
[70]	2022	DFCN	Reconstruction quality improved by eliminating aliasing effects utilizing correlation information between adjacent slices	Time-consuming and computationally expensive hyperparameter tuning, may lead to artifacts and noise
[71]	2022	HIWDNet	Achieved accurate cross-domain MRI reconstruction by leveraging image and wavelet domains. Efficiently reconstructed the structure while removing aliasing artifacts.	The complex architecture and intricate interactions of HIWDNet may hinder interpretability
[72]	2023	DSMENet	Enhanced detail and structure information, adapted to diverse MRI scenarios, and offered improved visual effects and generalization. Proved to be a competitive candidate for real-time MRI applications	Complex architecture and intricate interactions of DSMENet limit its interpretability
[73]	2023	SCU-Net	Achieved superior deghosting performance even at high acceleration factors, leading to high-quality complex MRIs	Relied on sparsified complex data and required further investigation into its effectiveness in handling complex anatomical structures and capturing fine details in highly undersampled MRI data
[61]	2023	RNLFNet	Effectively captured long-range spatial dependencies in the frequency domain, leading to enhanced MRI reconstruction	May have limitations when applied to parallel MRI and dynamic MRI
[74]	2023	GFN	Maintain more detailed MR images by capturing edge structures in gradient images	Lack of interpretability and explainability as black-box models, may lead to artifacts and noise

Architectures - Data Consistency and Unrolled Networks

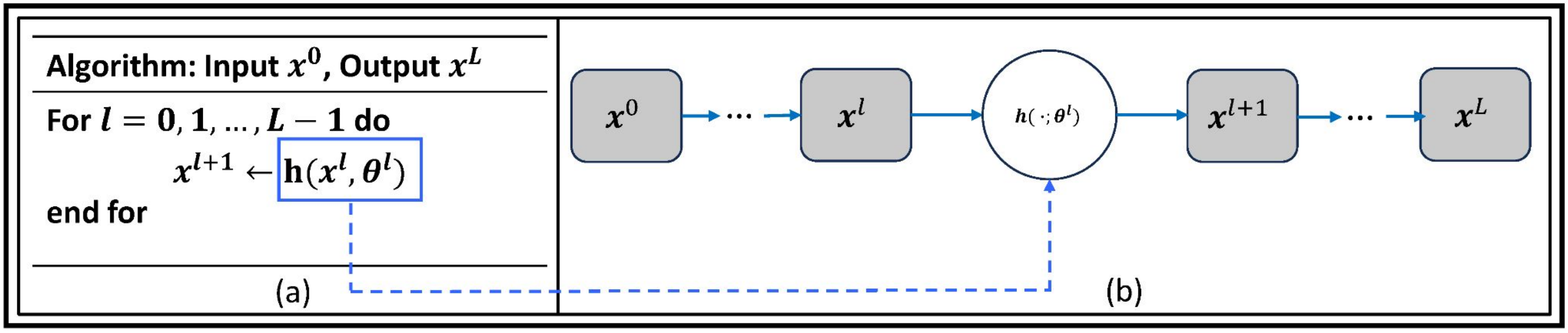

Unrolled networks: Mapping an Iterative Algorithm into a (a) Deep Network with (b) Trainable Parameters (in Blue) (adapted with changes from Monga, V.; Li, Y.; Eldar, Y.C. Algorithm unrolling: Interpretable, efficient deep learning for signal and image processing. IEEE Signal Process. Mag. 2021, 38, 18–44.

Architectures - Data Consistency and Unrolled Networks

Table 5. Data-Consistency Layers and Unrolled Networks-based MRI Reconstruction Models.

Ref.	Year	Network	Contributions	Unsolved Challenges
[33]	2018	VN	Preserved essential features of MR images, including pathologies not present in the training dataset	Suffer from residual artifacts that are particularly evident in the axial sequences
[34]	2018	VN	Provided rapid reconstruction speed of approximately 0.2 s per section	Variation in reconstruction times based on hardware models, the use of constant regularizations, and the absence of fully sampled data
[76]	2018	MoDL	Achieved faster convergence per iteration using numerical optimization blocks for data-consistency and required less training data	Use of many conjugate gradient steps in data-discrepancy layers may lead to increased computational time, possibly reducing reconstruction speed
[77]	2019	PC-CNN	Improved image accuracy by enforcing data consistency and enhanced convergence	Computational complexity, data dependency, limited interpretability, and sensitivity to noise and artifacts
[78]	2020	jVN	Image quality was improved, and blurring was reduced through the learning of efficient regularizers	Generalization to unseen data or different acquisition scenarios
[79]	2020	DeepcomplexMRI	No sensitivity information calculation required for resolving aliasing and channel correlations	High acceleration factors can result in persistent blurriness in the reconstructed MRIs
[80]	2020	Dense-RNN	Showed potential for capturing long-range dependencies among image units	Does not completely address the slow convergence issue inherent in proximal gradient descent methods
[81]	2020	TVINet	Ensured data consistency and preserved the fine details in the reconstructed MRI	Time-consuming and computationally expensive hyperparameter tuning, lack of uncertainty quantification in deterministic predictions
[82]	2020	FlowVN	Achieved accurate reconstructions of pathological flow in a stenotic aorta within a short timeframe of 21 s	Large training data requirement, interpretability
[83]	2022	CNN & UNet	Enhanced unfolding structures without complexity increase, using an adaptively calculated noise parameter for improved reconstruction performance	Suffer from training instability, slow convergence, and limited explainability, which can hinder its practical applicability and interpretability
[84]	2022	DEMO	Efficiently removed CS-MRI artifacts, such as motion, zebra, and herringbone artifacts	High computational requirements, including GPUs, for training and inference
[85]	2023	DIRCN	Used long-range skip connections to improve gradient and information flow	Model trained on retrospective public domain data, needs to be tested on clinically valid prospective data

DL Architectures - Learned Activations

Taken from [Hammernik, Kerstin, et al. "Learning a variational network for reconstruction of accelerated MRI data." Magnetic resonance in medicine 79.6 (2018): 3055-3071.]

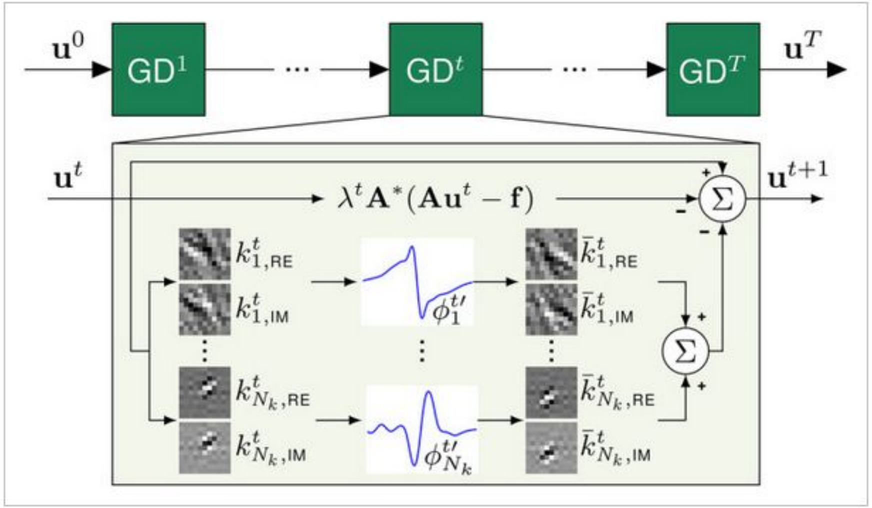

Figure 1 Open in figure viewer PowerPoint

Structure of the variational network (VN). The VN consists of T gradient descent steps. To obtain a reconstruction, we feed the undersampled k-space data, coil sensitivity maps and the zero filling solution to the VN. Here, a sample gradient step is depicted in detail. As we are dealing with complex-valued images, we learn separate filters k_i^t for the real and complex plane. The non-linear activation function $\phi_i^{t\prime}$ combines the filter responses of these two feature planes. During a training procedure, the filter kernels, activation functions and data term weights λ^t are learned.

DL Architectures - Attention

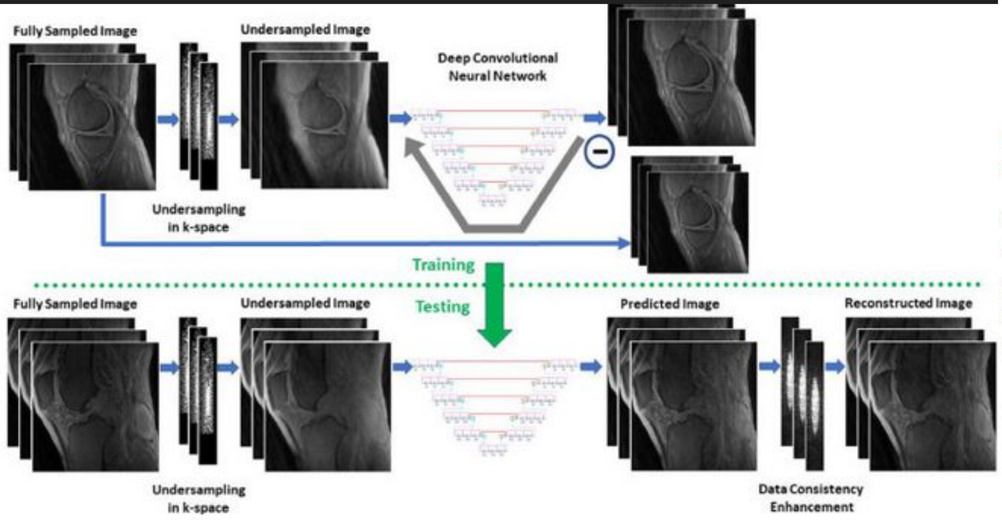

Download : Download high-res image (696KB)

Download : Download full-size image

[Wu, Yan, et al. "Self-attention convolutional neural network for improved MR image reconstruction." *Information sciences* 490 (2019): 317-328.]

Fig. 1. The workflow of employing the self-attention convolutional neural network (SAT-Net) for MR reconstruction. Fully sampled 3D images were retrospectively undersampled in *k*-space and transformed back to the image domain. In the training procedure, a convolutional neural network was established, in which loss was back-propagated and used to update model parameters iteratively. In testing, retrospectively undersampled images were passed through the well-trained network, and subsequent data consistency enforcement was performed to form the final reconstruction result.

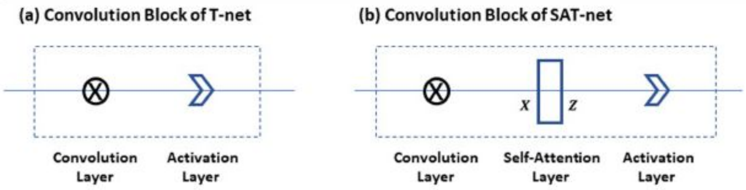

Download : Download high-res image (149KB)

Download : Download full-size image

Fig. 6. Comparison of the convolution block of a self-attention convolutional neural network with that of a traditional network. (a) Traditional convolution block without the self-attention mechanism incorporated, as used in the T-Net, and (b) novel convolution block with the self-attention mechanism incorporated, as used in the SAT-Net, which provides long-range dependencies.

[Kossaifi, Jean, et al. "T-net: Parametrizing fully convolutional nets with a single high-order tensor." Proceedings of the IEEE/CVF conference on computer vision and pattern recognition. 2019.]

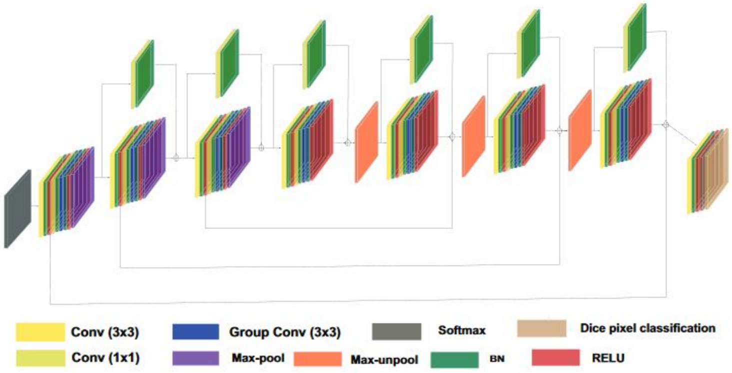

Figure 2: Diagram showing the structure of T-Net.

DL Methods - Plug and Play Priors

Pour Yazdanpanah, Ali, Onur Afacan, and Simon Warfield. "Deep plug-and-play prior for parallel MRI reconstruction." *Proceedings of the IEEE/CVF International Conference on Computer Vision Workshops*. 2019.

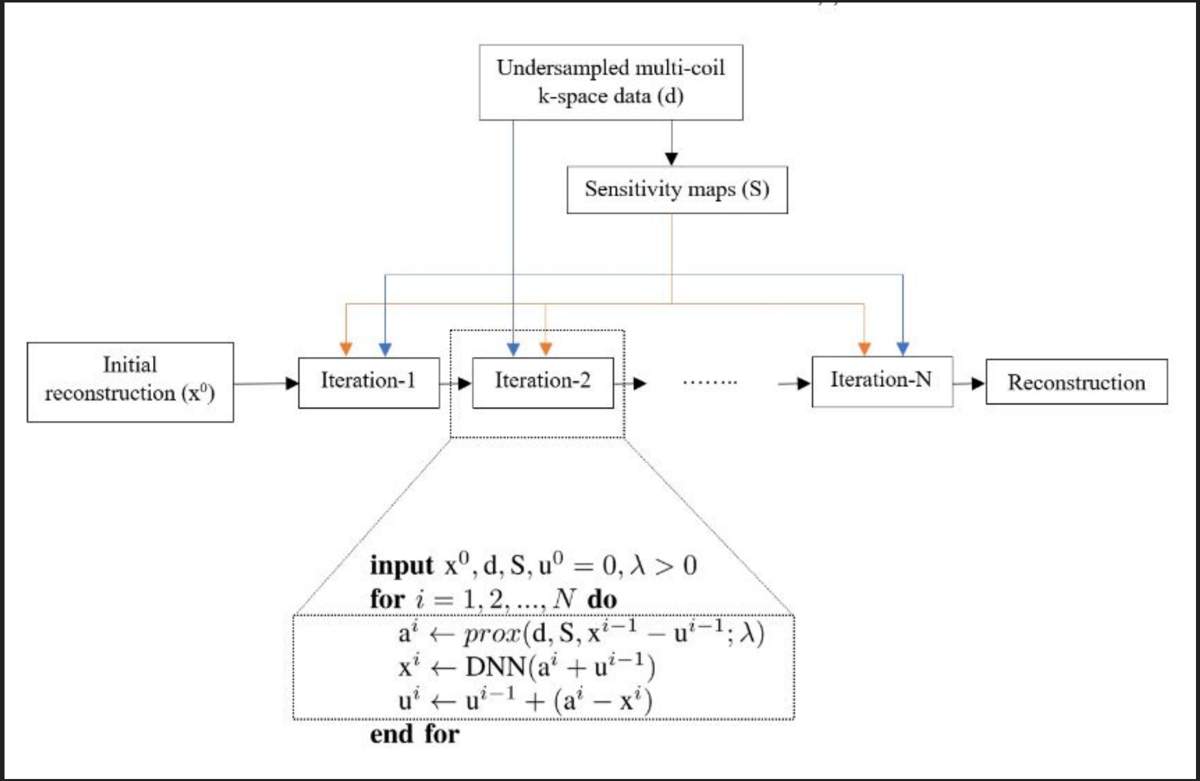

DL Methods - Diffusion Models

Chung, Hyungjin, and Jong Chul Ye. "Score-based diffusion models for accelerated MRI." *Medical image analysis* 80 (2022): 102479.

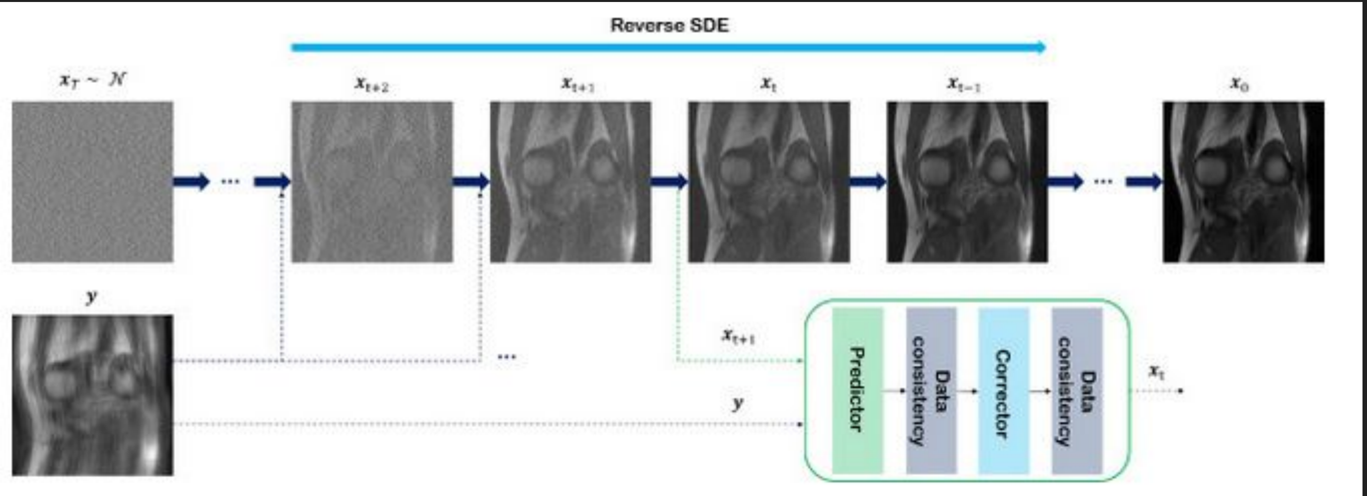

Download : Download high-res image (495KB)

Download : Download full-size image

Fig. 1. Overview of the proposed method. Starting from x_T, sampled from the prior distribution, x_0 is reached by solving the reverse SDE with score-based sampling, alternating between the update step, and the data consistency step.

Bayesian Methods

[Luo, Guanxiong, et al. "MRI reconstruction using deep Bayesian estimation." *Magnetic resonance in medicine* 84.4 (2020): 2246-2261.]

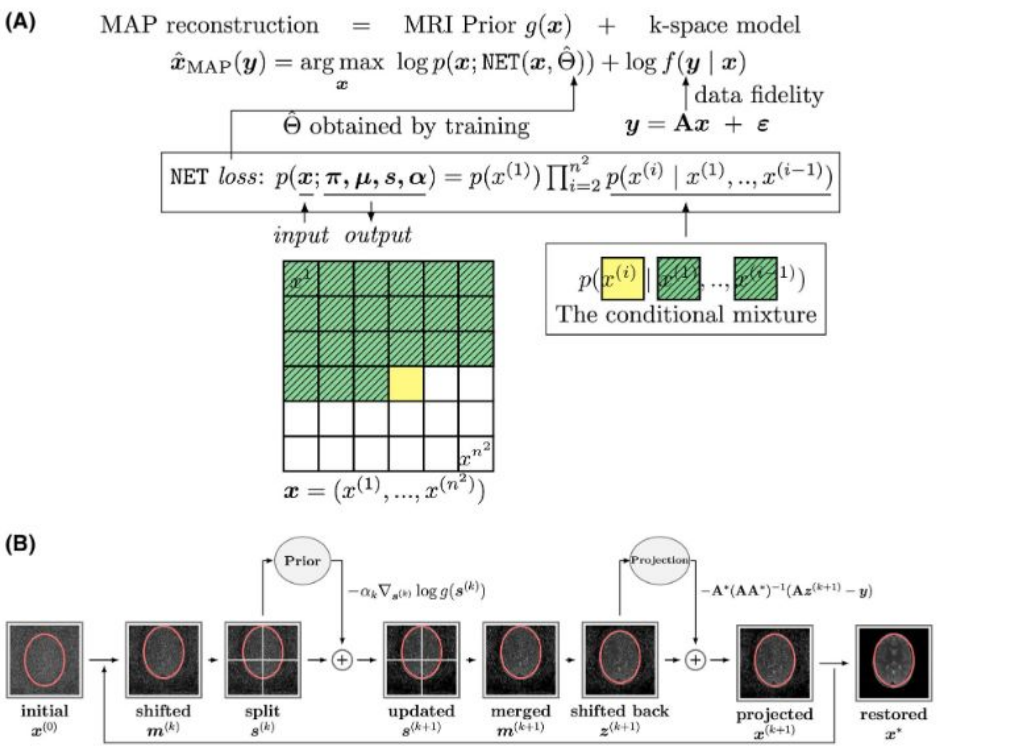

FIGURE 1 A, Overview of the MAP reconstruction. Conditional model in[13,14] defined the probability of image pixel (yellow) x_{ij} dependent on all the pixels from its up and left side (green). B, In this method, we reconstructed images with 256×256 matrix size, using the prior model $g(\boldsymbol{x})$ that was trained with 128×128 images and illustrated in Supporting Information Figure S1. To reconcile this mismatch, we split one 256×256 image into four 128×128 patches for applying the prior model. After updating $\boldsymbol{s}^{(k+1)}$, 4 patches for 1 image were merged to form an image with the original size of 256×256. Then the merged image was projected onto $\{\boldsymbol{x} | \boldsymbol{y} = \mathbf{A}\boldsymbol{x} + \boldsymbol{\varepsilon}\}$ in Equation (11). Furthermore, the random shift along phase encoding direction was applied to mitigate the stitching line in-between patches

Loss Functions

[Xuan, Kai, et al. "Multimodal MRI reconstruction assisted with spatial alignment network." *IEEE Transactions on Medical Imaging* 41.9 (2022): 2499-2509.]

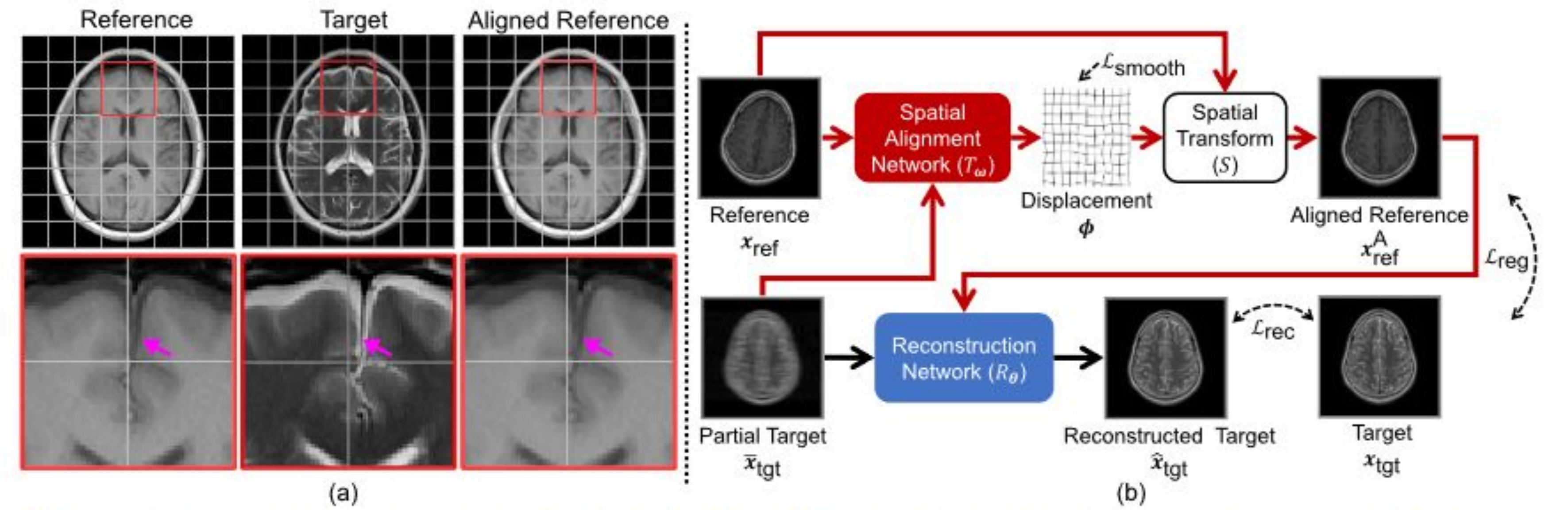

Fig. 1. A real case demonstrating the existence of spatial misalignment (a), and the overview of the proposed method (b). In (a), a real case of multi-modal MRI acquired for the diagnostic purpose demonstrates the existence of spatial misalignment (highlighted by arrows) between the reference (T1-weighted) and the target (T2-weighted) images. The aligned reference image is also available to show the effect of our proposed spatial alignment network. In (b), a spatial alignment network is integrated into the multi-modal MRI reconstruction pipeline to compensate for the spatial misalignment between the fully-sampled reference image and the under-sampled target. The data flow for the conventional deep-learning-based reconstruction is shown in black arrows, and the red arrows are for additional data flow related to our proposed spatial alignment network.

Adversarial Training

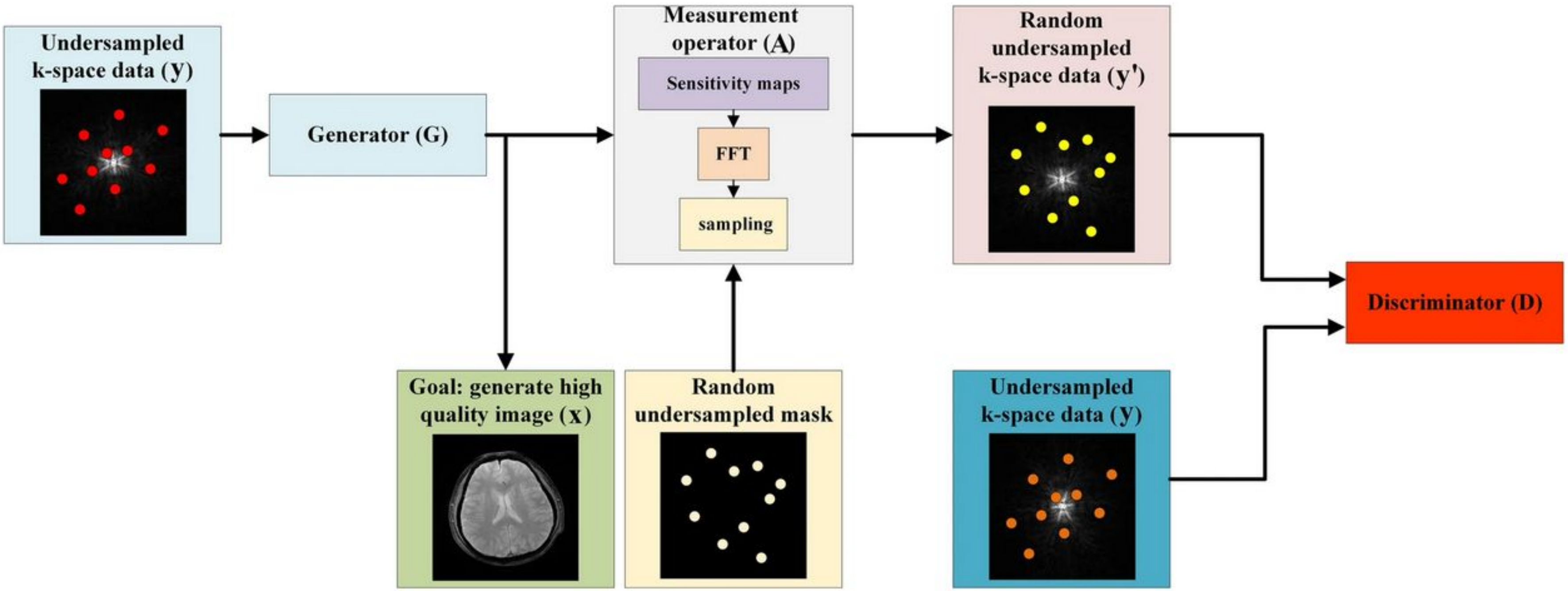

Unsupervised GAN learning system. The input and output of the generator is measurement complex-valued k-space data and two-dimensional image, then the output of generator performs forward measurement operation including a random undersampled mask to get simulation undersampled k-space data, finally, discriminator tries to distinguish between simulation data and measurement data. This figure is reproduced following Fig. 1 in Ref. [83]

From [Zeng, Gushan, et al. "A review on deep learning MRI reconstruction without fully sampled k-space." BMC Medical Imaging 21.1 (2021): 195.]

Self Supervised Learning

Figure 7. Self-Supervised Training Paradigm for Unrolled MRI Reconstruction Network: Regularizer (R) and Data Consistency (DC) Components (adapted with changes from [137]).

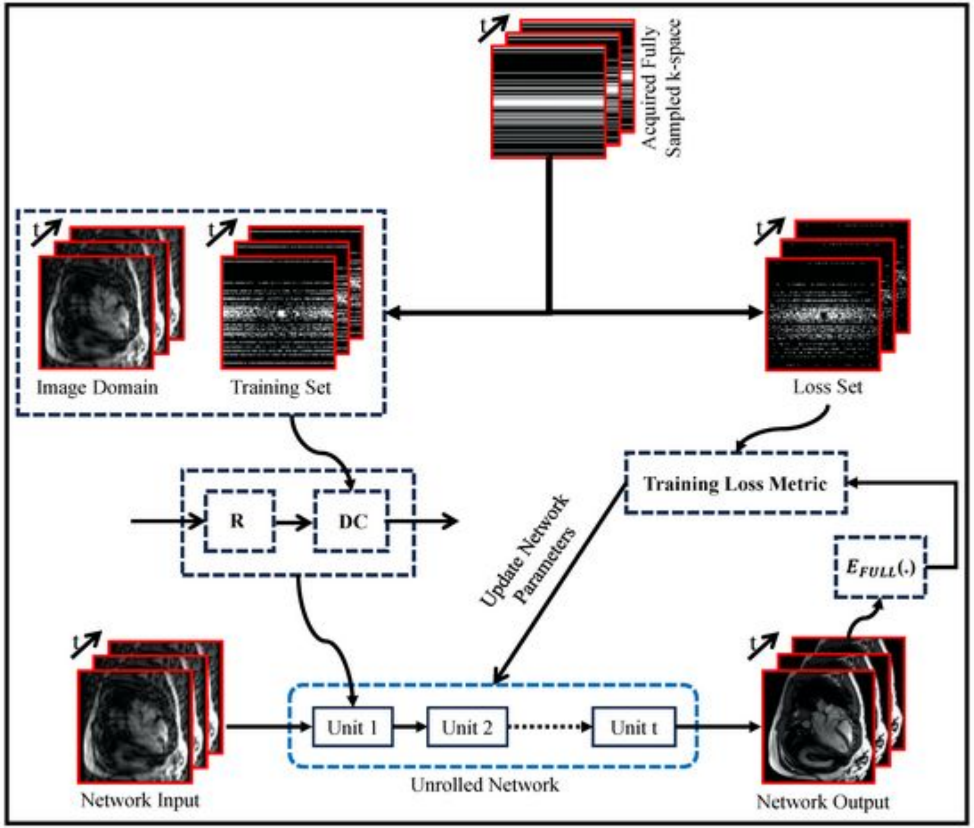

Dynamic MRI

From: CINENet: deep learning-based 3D cardiac CINE MRI reconstruction with multi-coil complex-valued 4D spatio-temporal convolutions

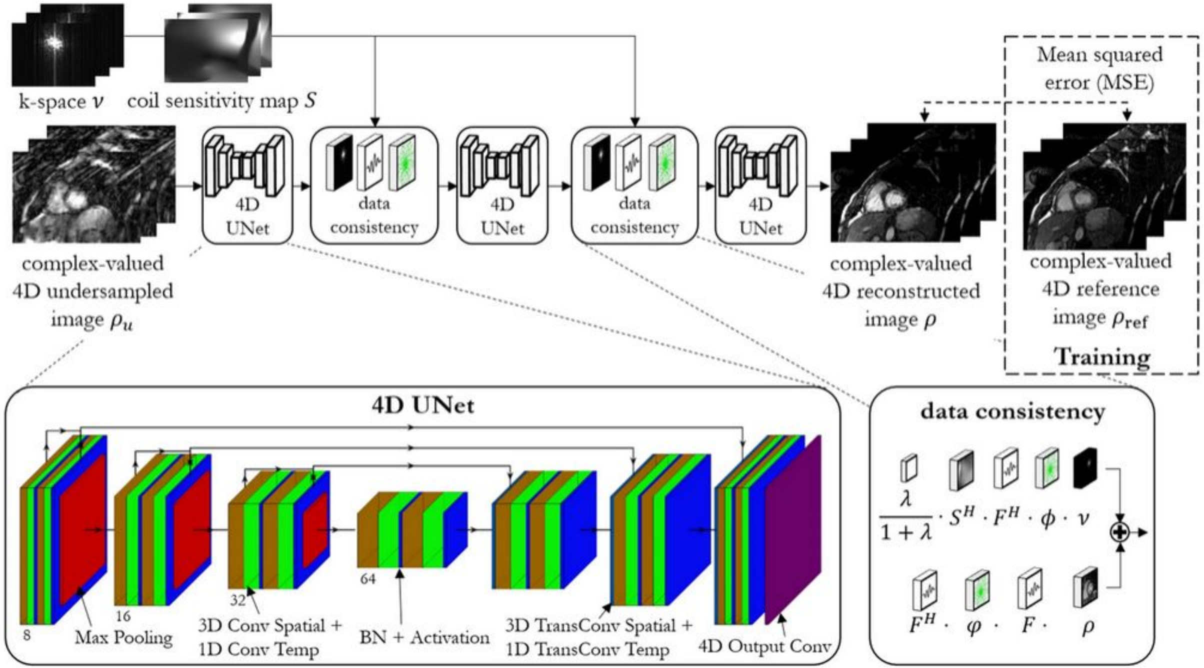

Proposed 4D CINENet resembles a proximal gradient algorithm with alternating 4D sparsity-learning UNet and data consistency blocks. The 4D UNet consist of an encoding and decoding branch with cascaded (3 + 1)D (3D + time) complex-valued convolutional layers, 3D convolution spatial (brown layer) + 1D convolution temporal (green layer), complex-valued batch normalization (BN) with rectified linear unit activation function (blue layer), max-pooling (encoder; red layer) and (3 + 1)D transposed complex-valued convolution (decoder; light blue layer). A final 4D complex-valued convolution compresses the complex-valued feature channels to a single complex-valued output channel (purple layer). Data consistency block receives as input the current reconstructed image ρ, the k-space ν, coil sensitivity map S, the subsampling mask ϕ and the regularization parameter λ. φ denotes the scaled subsampling mask. F represents the Fourier transformation and F^H the inverse Fourier transformation. The network is trained end-to-end with mean squared error loss between retrospective undersampled images ρ_u (3× to 8× and varying temporal resolution) and iterative SENSE reconstructed reference image ρ_{ref} (2.5×). Figure was created using TikZ 3.1.5.

Functional MRI

[Li, Xuesong, et al. "Deep residual network for highly accelerated fMRI reconstruction using variable density spiral trajectory." *Neurocomputing* 398 (2020): 338-346.]

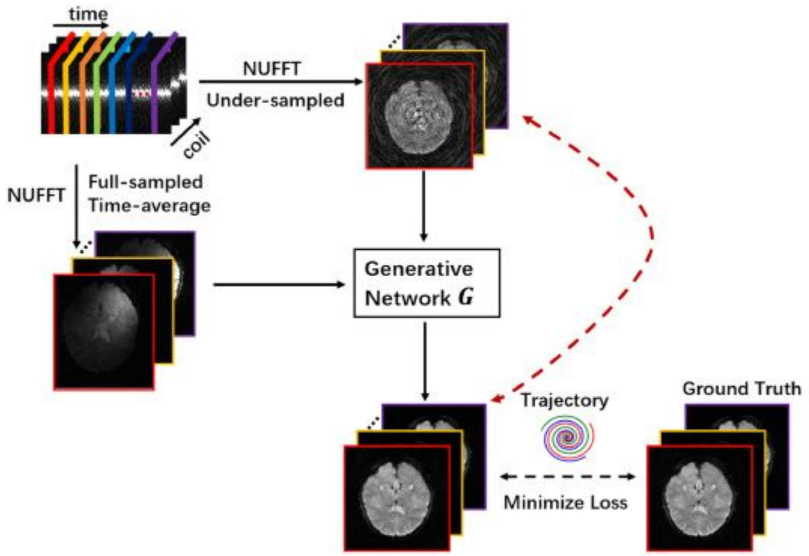

Download : Download high-res image (345KB)

Download : Download full-size image

Fig. 2. Overview of the proposed deep learning method. Both aliasing images and reference images are used as the input of the network which is trained to map the full-sampled reconstruction image.

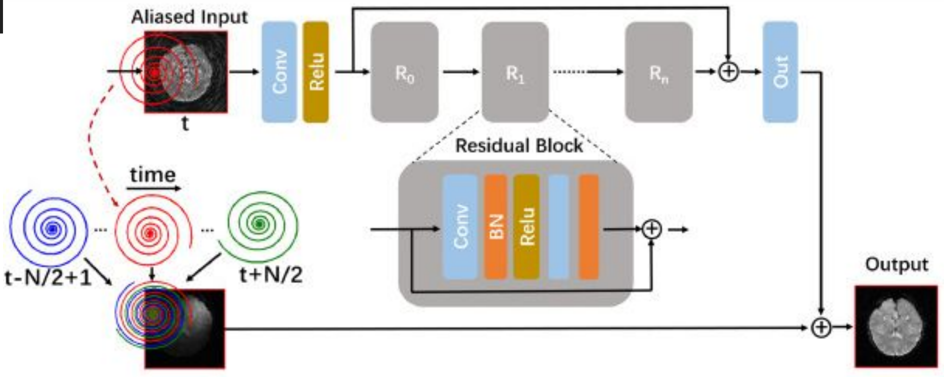

Download : Download high-res image (333KB)

Download : Download full-size image

Fig. 3. Network architecture used for this study. The network built by stacking several residual blocks can grasp dynamic information from under-sampled k-space data. The final result is obtained by adding the reference image to the output.

Functional MRI

[Taneja, Karan, et al. "A Bayesian Deep CNN Framework for Reconstructing kt-Undersampled Resting-fMRI." *2020 25th International Conference on Pattern Recognition (ICPR)*. IEEE, 2021.]

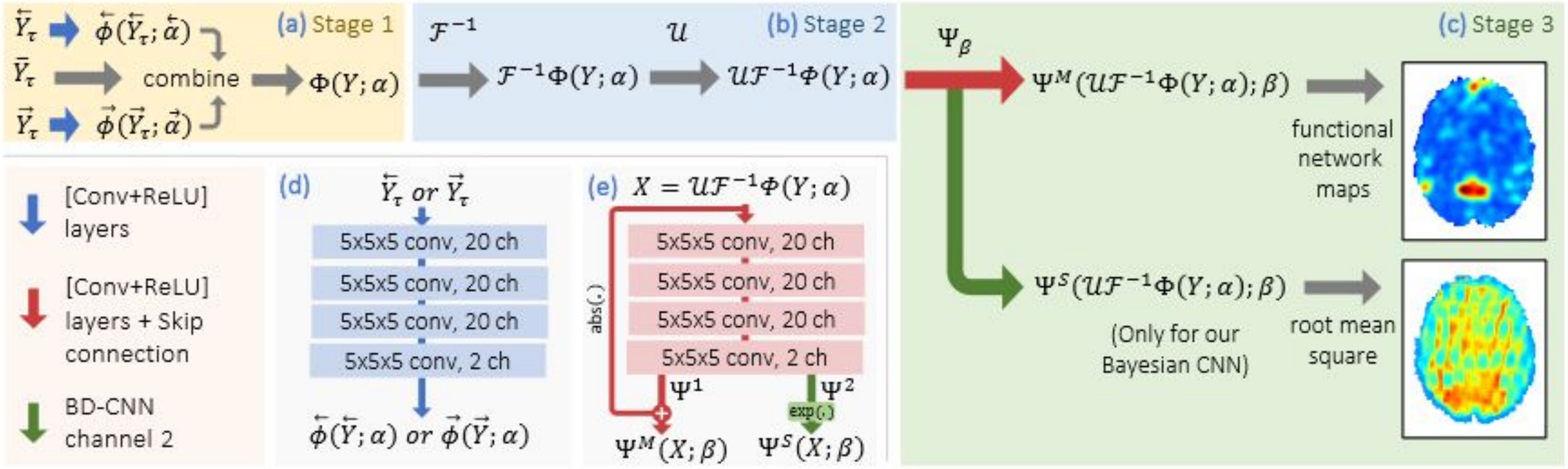

Fig. 2: **Our Convolutional Neural Network Framework.** The end-to-end CNN framework has 3 stages where (i) the first stage fills in missing k-space data, (ii) the second stage applies the inverse Fourier transform and performs temporal interpolation and (iii) the last stage performs spatiotemporal image quality enhancement. All variants are described in Section II-E.

Challenges and Shortcomings

Table 11. Shortcomings and Mitigation Strategies of DL-based MRI Reconstruction Models.

Shortcoming	Description	Mitigation Strategies
Data Dependency [205,206]	DL models require large labeled training datasets, which may be challenging to obtain, limiting model generalization.	Data augmentation, transfer learning, and domain adaptation techniques can address data scarcity and improve generalization.
Limited Generalization [205,207,208]	Models trained on specific datasets may not perform well on data from different scanners or protocols due to variations in imaging characteristics.	Domain adaptation, model ensemble techniques, and domain-specific regularization methods can enhance generalization across different imaging settings.
Black Box Nature and Limited Explainability [209,210]	DL models lack transparency, interpretability, and the ability to provide detailed explanations for their predictions or reconstruction outputs.	Explainable AI techniques, such as attention mechanisms, interpretability methods, and integration with clinical knowledge or rule-based models, can enhance interpretability and provide explainable outputs.
Computational Resource Requirements [211,212,213]	Training and deploying DL models for MRI reconstruction can be computationally demanding, limiting accessibility in clinical settings.	Model compression techniques, efficient network architectures, and hardware acceleration can help alleviate computational resource requirements.
Susceptibility to Adversarial Attacks [214,215]	DL models can be vulnerable to adversarial attacks, raising concerns about their robustness and reliability.	Adversarial training, input preprocessing (e.g., denoising, smoothing), and defensive mechanisms (e.g., detection, certification) can enhance model robustness against adversarial attacks.
Handling Artifacts and Novel Cases [119,216]	DL models may struggle with complex artifacts that differ significantly from the training data distribution.	Augmenting training data with diverse artifacts, using data-specific loss functions, and incorporating domain knowledge can improve model performance on artifacts.
Hyperparameter Tuning [217,218]	The performance of DL models is sensitive to hyperparameter settings, requiring careful tuning.	Automated hyperparameter tuning techniques (e.g., grid search, Bayesian optimization) and model-specific optimization strategies including metaheuristics can enhance model performance through effective hyperparameter tuning.

Discussion